

August 2014

Effects of Ball Milling and Sintering on Alumina and Alumina-Boron Compounds

Thomas Cross

University of Wisconsin-Milwaukee

Follow this and additional works at: <https://dc.uwm.edu/etd>

 Part of the [Materials Science and Engineering Commons](#)

Recommended Citation

Cross, Thomas, "Effects of Ball Milling and Sintering on Alumina and Alumina-Boron Compounds" (2014). *Theses and Dissertations*. 493.
<https://dc.uwm.edu/etd/493>

This Thesis is brought to you for free and open access by UWM Digital Commons. It has been accepted for inclusion in Theses and Dissertations by an authorized administrator of UWM Digital Commons. For more information, please contact open-access@uwm.edu.

EFFECTS OF BALL MILLING AND SINTERING ON ALUMINA AND ALUMINA-BORON COMPOUNDS

by

Thomas Cross

A Thesis Submitted in

Partial Fulfillment of the

Requirements for the Degree of

Master of Science

in Engineering

at

The University of Wisconsin-Milwaukee

August 2014

ABSTRACT

EFFECTS OF BALL MILLING AND SINTERING ON ALUMINA AND ALUMINA-BORON COMPOUNDS

by

Thomas Cross

The University of Wisconsin-Milwaukee, 2014
Under the Supervision of Professor Ben Church

Alumina has a wide variety of applications, but the processing of alumina based materials can be costly. Mechanically milling alumina has been shown to enhance the sintering properties while decreasing the sintering temperature. Additions of boron have also proven to increase sintering properties of alumina. These two processes, mechanical milling and boron additions, will be combined to test the sintering properties and determine if they are improved upon even further compared to the individual processes.

Multiple samples of pure alumina, 0.2 weight percent boron, and 1.0 weight percent boron are batched and processed in a ball mill for different time intervals. These samples are then characterized to observe the structure and properties of the samples after milling but before sintering. Pellets are dry pressed from the milled powders, sintered at 1200°C for one to 10 hours, and characterized to determine the impact of processing.

X-ray diffractometry (XRD) was used on each sample to determine crystallite size and lattice parameters at different stages throughout the experiment. XRD was also used to identify any samples with an aluminum borate phase. Scanning electron microscopy

(SEM) was used to observe the powder and pellet morphology and to measure bulk chemical composition. Samples were sputter coated with an Au-Pd coating observed in the SEM to characterize the topography as a function of variables such as milling time, boron composition, and sintering time. Additionally, porosity and change in diameter were measured to track the sintering process.

Milling sample for longer periods of time would be unnecessary due to the crystallite size leveling off between 10 and 12 hours of milling time. Samples of alumina with 0.2 weight percent boron prove to have very little effect on the sintering properties. At 1.0 weight percent boron, there are changes in diffraction patterns and topography after being sintered for one hour. The porosities of all of the sintered samples are larger than anticipated likely due to a poor sinter. Higher boron compositions appear to have the greatest effect on post sintering properties by producing the smallest relative porosities and largest changes in densification.

Reduction of crystallite size during high-energy ball milling is independent of boron composition in the range of compositions that were investigated. The lattice parameters of the main alumina phase as a function of milling time did not follow the same trends shown in literature, indicating any impurities within the literature samples affected the lattice parameter measurements. Increased milling times on the samples that contain 1.0 weight percent boron are observed to have a higher densification during sintering. Higher boron additions increase the densification from sintering while maintaining a relatively lower porosity. Relative to the other samples, the highest sample densification is observed from both 1.0 weight percent boron additions and ball milling for 12 hours and sintering for one and 10 hours.

TABLE OF CONTENTS

Abstract.....	ii
Table of Contents	iv
List of Figures.....	v
List of Tables	viii
Acknowledgements	ix
1. Introduction.....	1
2. Background	3
2.1 Sintering	3
2.2 Doping.....	6
2.3 Ball Milling.....	8
3. Experimental Procedures	14
3.1 Sample Preparation	14
3.1.1 Ball Milling.....	15
3.1.2 Sintering.....	16
3.2 Characterization Techniques.....	18
3.2.1 X-ray Diffraction (XRD)	18
3.2.2 Scanning Electron Microscope (SEM)	19
3.2.3 Porosity	20
4. Experimental Results.....	22
4.1 XRD	22
4.2 SEM	35
4.3 Porosity	46
5. Conclusions.....	53
6. Future Work.....	56
7. References	58

LIST OF FIGURES

Figure 1:	Phase diagram – Aluminum rich side of Al-B.....	4
Figure 2:	Phase diagram – Al_2O_3 - B_2O_3	4
Figure 3:	The crystal structure of corundum (Al_2O_3) (a) Corundum structure in α - Al_2O_3 (b) Top view of structure (c) Octahedral structure of α - Al_2O_3	5
Figure 4:	Lattice Parameters (a) and (c) of Al_2O_3 as a Function of Milling Time	6
Figure 5:	Phase diagram – MnO - Al_2O_3	7
Figure 6:	The three stages during ball milling: (a) the Rittinger stage, (b) the aggregation stage, and (c) the agglomeration stage	10
Figure 7:	X-ray diffraction pattern of corundum at various milling times.....	12
Figure 8:	Grain size of corundum vs. milling time	13
Figure 9:	Press used to create pellets for sintering	16
Figure 10:	Die used to create pellets, disassembled	17
Figure 11:	Furnace used to sinter pellets	17
Figure 12:	(Left) Scale setup used to make weight measurements for porosity (Right) Basket used to suspend pellets in second weight measurement	21
Figure 13:	The samples selected to be analyzed after sintering	21
Figure 14:	XRD pattern of sample of 0.2 wt% boron	22
Figure 15:	1.0 wt% boron before sintering.....	25
Figure 16:	1.0 wt% boron before sintering from 30° to 55° 2θ	25
Figure 17:	0.2 wt% boron milled for 12 hours	26
Figure 18:	0.2 wt% boron milled for 12 hours from 30° to 55° 2θ	26
Figure 19:	1.0 wt% boron milled for 12 hours	27
Figure 20:	1.0 wt% boron milled for 12 hours from 30° to 55° 2θ	27

Figure 21:	Samples milled for 12 hours, sintered for 1 hour.....	28
Figure 22:	Samples milled for 12 hours, sintered for 1 hour from 30° to 55° 2θ.....	28
Figure 23:	Crystal properties vs. milling time – Before sintering.....	31
Figure 24:	Crystal properties vs. milling time of 1.0 wt% boron samples – After sintering	32
Figure 25:	Crystal properties vs. composition of 12-hour milled samples – After sintering	33
Figure 26:	Components as-received at 200x and 1000x magnification (a) Alumina at 200x, (b) Alumina at 1000x, (c) Boron at 200x, (d) Boron at 1000x	35
Figure 27:	Samples of 1.0 wt% boron milled for various amounts of time at 200x magnification (a) Hand Mixed, (b) 0.3 hours, (c) 3 hours, (d) 6 hours, (e) 12 hours.....	37
Figure 28:	Samples milled for 12 hours before sintering at 1000x magnification (a) Pure Al ₂ O ₃ , (b) 0.2 wt% boron, (c) 1.0 wt% boron.....	38
Figure 29:	Al ₂ O ₃ milled for 12 hours at 1000x magnification (a) Before sintering, (b) Sintered for 1 hour, (c) Sintered for 10 hours	39
Figure 30:	0.2 wt% Boron Milled for 12 hours at 1000x magnification (a) Before Sintering, (b) Sintered for 1 hour, (c) Sintered for 10 hours.....	40
Figure 31:	1.0 wt% boron milled for 12 hours at 1000x magnification (a) Before sintering, (b) Sintered for 1 hour, (c) Sintered for 10 hours.....	42
Figure 32:	Samples milled for 12 hours and sintered for 1 hour at 1000x magnification (a) Pure alumina, (b) 0.2 wt% boron, (c) 1.0 wt% boron ...	43
Figure 33:	1.0 wt% boron, hand mixed, sintered for 1 hour at 200x magnification ...	45
Figure 34:	Approximate upper-right of Figure 33 at 1000x magnification Rod-like features exclusive to this sample.....	45
Figure 35:	Change in diameter vs. porosity of samples after sintering	48
Figure 36:	Porosity vs. milling time of 1.0 wt% boron samples after sintering for 1 hour	49

Figure 37:	Porosity vs. composition of samples milled 12 hours after sintering for 1 and 10 hours	50
Figure 38:	Change in diameter vs. milling time of 1.0 wt% boron samples after sintering for 1 hour.....	51
Figure 39:	Change in diameter vs. composition of samples milled for 12 hours after sintering for 1 and 10 hours	52

LIST OF TABLES

Table 1:	Table of original samples. Sample 15 was hand mixed.....	15
Table 2:	The samples selected for further analysis after sintering.....	18
Table 3:	Calculated Crystallite Size from Various Sources. Sample 19 was hand mixed.....	34
Table 4:	Porosity of sintered samples *Diameter before sintering is assumed to be 12.7mm.....	47

ACKNOWLEDGEMENTS

I wish to thank Dr. Sudeep Ingole for providing the idea and framework of this experiment. Without him, this work would not have happened.

I would also like to thank my advisor, Dr. Ben Church for everything he has done throughout this entire process from ordering the materials to training me on whatever I needed to be trained on. I would not be anywhere with this work without his guidance and patience.

I would also like to thank Dr. Steve Hardcastle for allowing me use of the Advanced Analytical Facility and for the training on the instruments used.

To my fiancée, Jessica: Thank you for dealing with me throughout this whole process and supporting me whenever I needed it.

1. Introduction

The use of alumina in different engineering applications is already widespread due to its many beneficial properties. Some of these applications include, but are not limited to: cutting and grinding tools, biomedical implants, high temperature insulation, fire retardants, as a catalyst in high temperature reactions, reinforcements in metals, ceramics, and polymer matrix composites. The reason alumina can be used in such a wide variety of applications is because it has low density, good chemical resistance and electrical insulation, low thermal conductivity, high hardness, good mechanical strength, and good wear resistance [1, 2]. Alumina is normally processed by sintering. Performance of materials is generally enhanced by high densities and absence of defects [3]. By adding second phases, these properties can be improved by increasing densification while lowering sintering difficulties [1, 2].

Boron is another material with many good properties that make it useful in several industrial applications. It has a high melting point of 2076°C, a Knoop hardness between 2160 and 2900, and a high Young's modulus. Boron also has a low density of 2.340 g/cm³. These properties along with its high melting temperature are what make boron an appealing element for use in nanotechnology applications like nanoelectronic devices and boron neutron capture theory (BNCT), which is currently one of the most promising methods of cancer treatment. Boron compounds, on the nano-scale, such as boron nitride and boron carbide are already being used in applications such as preparation for space shuttle coatings and field emission devices, respectively [4].

Alumina and aluminum borates have also been looked at for nanotechnology applications. These ceramics have enhanced mechanical properties and chemical

stability, a low coefficient of thermal expansion, a high tensile strength, and can potentially be used in high temperature composite applications [5-7]. Nanowires, also known as whiskers, have been a large topic of interest as of late, specifically as a strengthening material in composites [6]. Aluminum borate is one material that has been investigated because it has many advantages over one of the more commonly used materials, silicon carbide. Aluminum borates do not readily oxidize at higher temperatures, like SiC does, and they can also be produced between one-tenth and one-twentieth of the cost [6, 7]. A problem with aluminum borate whiskers, however, is that they will react with the aluminum matrices which will cause the tensile strength of composites to drop significantly [7].

Current production of the materials for these applications is rather expensive. Alumina is normally sintered at 1700°C. These high sintering temperatures and long cycle times lead to high costs of processing [8]. By increasing the densification of alumina, it allows sintering at lower temperatures and at shorter cycles, which result in reduced production costs [3].

Goodshaw et al. showed that by mechanically milling alumina, the sintering temperature would drop significantly [8]. Paluri and Ingole also show that small additions (one to three percent) of boron to alumina can improve sintering properties [2]. By both ball milling and adding small amounts of boron to the material, the sintering temperature may be able to be reduced and, in turn, reduce the cost of production of these kinds of material. The combination of mechanical milling and simultaneous boron additions has not yet been investigated. This work is the first work to analyze what happens when both processing variables are introduced.

2. Background

2.1 Sintering

Compacted alumina is normally sintered at about 1700°C in order to gain high densities in alumina components. There are a few ways to drop this temperature, one being doping and the other being ball milling. There are many advantages to be gained when sintering alumina at lower temperatures such as lower costs, finer grain sizes, and the ability to co-fire alumina with other materials of a lower melting point [8].

Boron forms borides with many different metals like aluminum, titanium, and tungsten. These borides have been shown to have higher strengths and hardnesses than their respective single-phase materials [1]. Figures 1 and 2 are phase diagrams of Al-B and Al_2O_3 - B_2O_3 , respectively. Figure 1 shows that AlB_2 can form at lower temperatures and at lower compositions of boron. This phase is desirable due to its higher hardness (~15 GPa) than 99% pure alumina (9 to 12 GPa). This phase has also been shown to improve hardness and toughness in ceramics [1].

Figure 2 shows the different aluminum borate compounds. The two most favorable compounds are $\text{Al}_4\text{B}_2\text{O}_9$ or $\text{Al}_{18}\text{B}_4\text{O}_{33}$. These are the most favorable because they are economical and their high strength, high modulus, and low thermal expansion coefficients. The reported temperature for $\text{Al}_{18}\text{B}_4\text{O}_{33}$ whiskers is 1400°C [1].

Paluri and Ingole's XRD analysis show that both $\text{Al}_4\text{B}_2\text{O}_9$ and $\text{Al}_{18}\text{B}_4\text{O}_{33}$ are formed with all composites of boron (1, 2, and 3 wt%) when sintered at 1200°C but the $\text{Al}_{18}\text{B}_4\text{O}_{33}$ phase was not stable when sintered at 1500°C [1, 2].

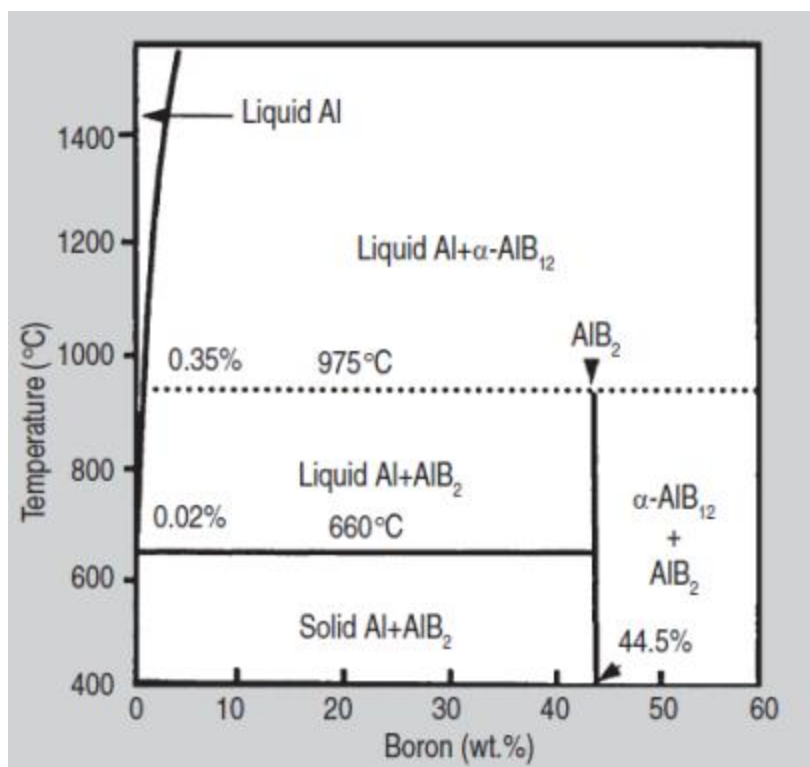


Figure 1: Phase diagram – Aluminum rich side of Al-B [1]

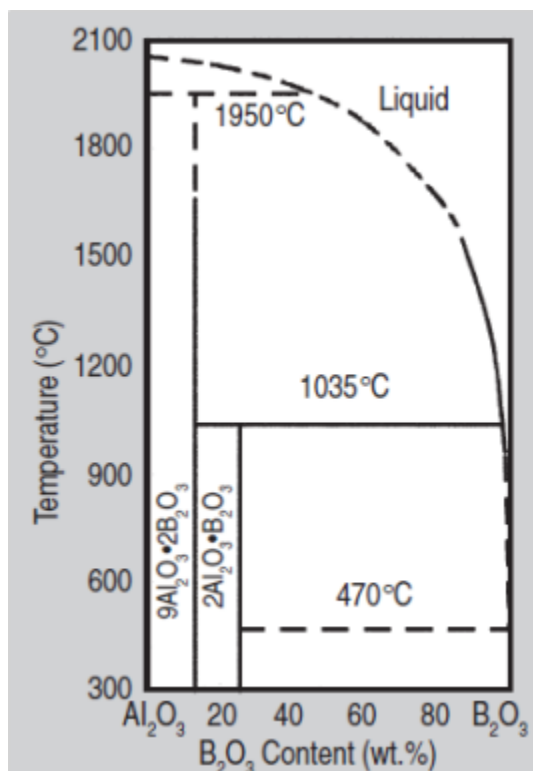


Figure 2: Phase diagram – Al₂O₃-B₂O₃ [1]

Figure 3 shows the crystal structure of corundum. Ideally, the crystal structure of $\alpha\text{-Al}_2\text{O}_3$ consists of closely packed A and B planes with large oxygen anions stacked in the sequence as shown in Figure 3 (a). Since the alumina cations have a valence of +3 and the oxygen anions have a valence of -2, there can only be two cations per three anions to maintain electrical neutrality. The cations only occupy two-thirds of the octahedral structure [9].

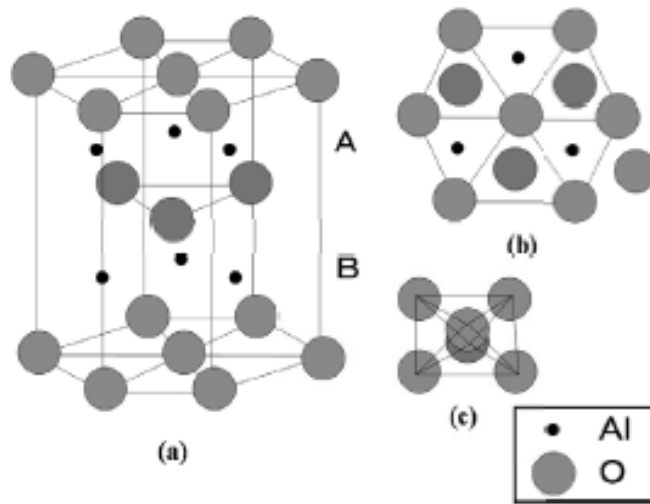


Figure 3: The crystal structure of corundum (Al_2O_3)
 (a) Corundum structure in $\alpha\text{-Al}_2\text{O}_3$ (b) Top view of structure
 (c) Octahedral structure of $\alpha\text{-Al}_2\text{O}_3$ [9]

The dependence of lattice parameters (a) and (c) versus milling time are shown in Figure 4. After milling and sintering, the lattice expands, but alumina remains in the $\alpha\text{-Al}_2\text{O}_3$ form, perhaps due to vacancies or other defects [8]. Figure 4 shows that lattice parameter (a) is steadily increased until eight hours of milling, but starts to decrease

afterwards, whereas lattice parameter (c) is steadily increased up to eight hours of milling, then increased at a much shallower slope after eight hours.

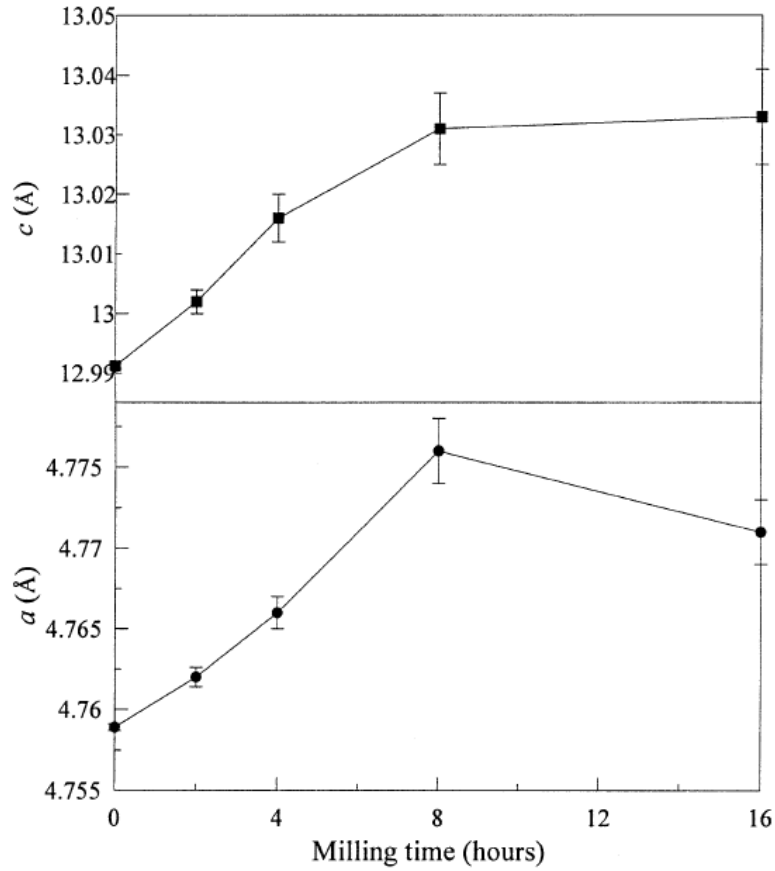


Figure 4: Lattice Parameters (a) and (c) of Al_2O_3 as a function of milling time [8]

2.2 Doping

It is widely known that by adding dopants to alumina, or starting with a very fine particle size, that the sintering temperature can be reduced by up to several hundred degrees. Doping alumina for the purpose of sintering temperature reduction usually

means the addition of oxides. This addition of oxides is usually less than 1%, but it can sometimes be as high as 3%. For example, dense alumina can be sintered well below 1700°C with small additions of MnO [10]. Figure 5 shows a phase diagram of a MnO- Al_2O_3 system that forms a eutectic at 1520°C. TiO_2 , Cu_2O , CaO , and SiO_2 are also known to reduce the sintering temperature in alumina. These dopants are beneficial because they can decrease the densification temperature either by forming a grain boundary film of liquid eutectic or by creating defects that enhance the bulk diffusion rates. If combinations of dopants are added, the densities have been reported to be higher [8]. For example, the alumina-calcia-silica system forms liquid silicates and has many eutectics within the temperature range of 1200-1400°C, with the lowest being 1170°C [10]. When dopants are added, there is sometimes a detrimental effect to the physical and chemical properties of alumina [8].

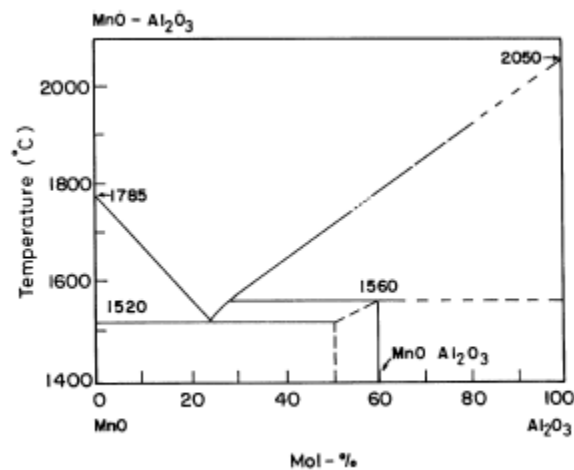


Figure 5: Phase diagram – MnO- Al_2O_3 [10]

2.3 Ball Milling

Mechanical milling is commonly used to synthesize noncrystalline metals, alloys, intermetallic compounds, ceramics, composites, and nanocomposites. By milling in reactive atmospheres, mechanical milling can also be used to produce various intermetallics and nanocomposites in-situ [11].

When ball milling, the starting powder gets trapped between the highly kinetic milling balls and the inside surface of the vial. This causes repeated deformation, rewelding, and fragmentation of the starting powder. This causes the formation of fine, dispersed particles in the grain-refined matrix [12]. By milling, the surface area of the powder is increased along with a chance to dramatically increase the number of regions of high activity in the surface [13]. Presently, the processes occurring in grinding machines are *coarse grinding*, where particle size is decreased, *fine grinding*, further particle size decrease and aggregation of particles, *densification of aggregates and deconstruction of their constituent grains*, where aggregate microstructure is refined and particle welding takes place, and *recrystallization of the primary particles*, where grinding of aggregates and recrystallized particles takes place. [14]. It is expected that powders that contain a large number of internal voids grind down much better than powders that are void free, due to the internal voids acting as fracture initiation sites [15].

Nanometer sized particles have been produced by high energy mechanical milling in many materials, including alumina. These milled powders have been shown to have enhanced sintering kinetics, which allow 92% dense materials with fine grains to form after sintering between only 1200°C and 1270°C, which is even lower than the 1400°C sintering temperature that was seen using the doping method [8].

Two problems commonly occur when ball milling, however, one being contamination and the other being agglomeration. Since alumina has a high hardness, there is the possibility of contamination coming from the milling media. In many journal publications, researchers will acknowledge possible sources of contamination but will usually ignore it. The other problem, agglomeration, can cause uneven sintering in the milled product. This causes the sintered product to sometimes be mechanically weak and porous. Inside agglomerates, alumina powder particles are known to increase the size of pores in the compact. Increases in the pore size decrease the densification rate. Agglomeration needs to be controlled in order to get the highest density compacts [8].

Ball milling has been shown to have three distinct stages: the Rittinger stage, the aggregation stage, and the agglomeration phase [13]. Figure 6 displays these stages graphically.

In the Rittinger stage, the interaction of particles can be neglected and the energy input is approximately proportionate to the new surface area formation.

In the aggregation stage, the new surface area is produced but is not proportional to the energy input because of the particle interaction. The degree of dispersion is still increasing and particles adhere to each other. The adhesion does not change the structure of the material.

In the agglomeration stage, the degree of dispersion drops a negligible value and then stops completely. It is possible that the particle interaction causes a decrease in surface area. Most of the mechanochemical reactions and changes that take in the crystal structures occur in this stage.

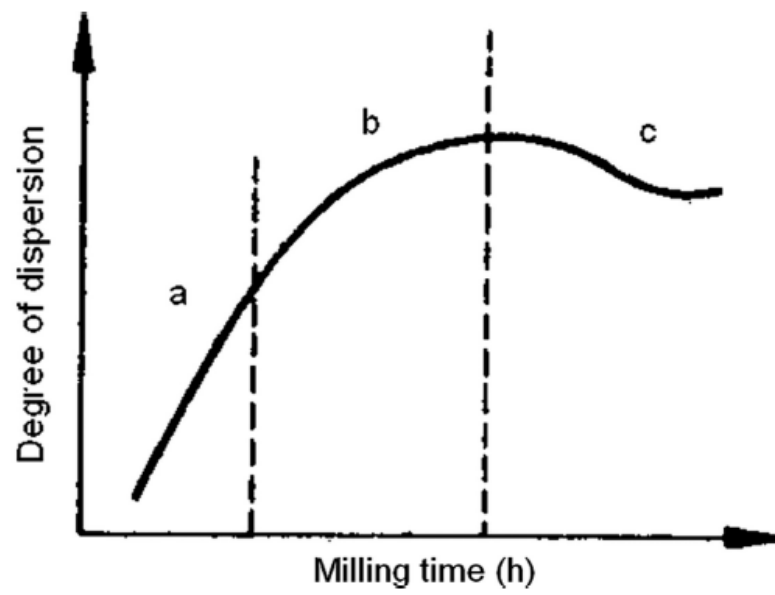


Figure 6: The three stages during ball milling: (a) the Rittinger stage, (b) the aggregation stage, and (c) the agglomeration stage [13]

Figure 7 shows the change in a XRD peak of corundum as a function of mechanical milling time. Mechanically milling the sample shows a broadening of the peaks with a decrease in intensity. Peak broadening from small crystallite sizes comes from the full-width at half maximums (FWHM) becoming larger. The Scherrer equation explains this trend. The Scherrer equation is as follows:

$$\tau = \frac{K\lambda}{\beta \cos \theta} \quad (\text{Eq. 1})$$

where τ is mean crystallite size, K is dimensionless shape factor (assumed as 0.9 for this work), λ is the x-ray source wavelength, β , sometimes denoted as $\Delta(2\theta)$, is broadening at FWHM, and θ is the Bragg angle. The equation shows that the mean crystallite size is inversely proportional to the peak broadening. Therefore, as peaks are broadened, the average crystallite size is decreased. Conversely, narrower peaks are a result of a larger crystallite size.

The grain sizes in Figure 7 start from about 350 nm (most narrow peaks) for the unmilled samples and become reduced to about 13 nm (most broad peaks) after 60 hours of milling [16].

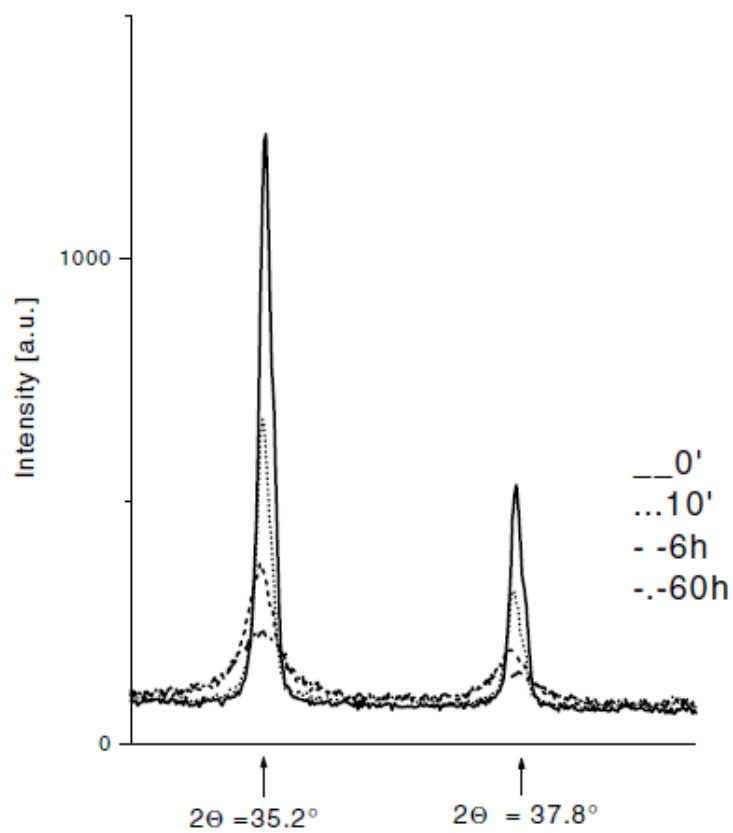


Figure 7: X-ray diffraction pattern of corundum at various milling times [16]

Figure 8 proves the grain sizes previously mentioned. It also shows the grain size decrease leveling off between about 500 minutes and 1750 minutes of milling. This kind of trend allows the milling time to be decreased while still maximizing the amount the crystal size is decreased during processing. After two hours of milling, the grain size is reduced to roughly one-tenth of the starting value [16].

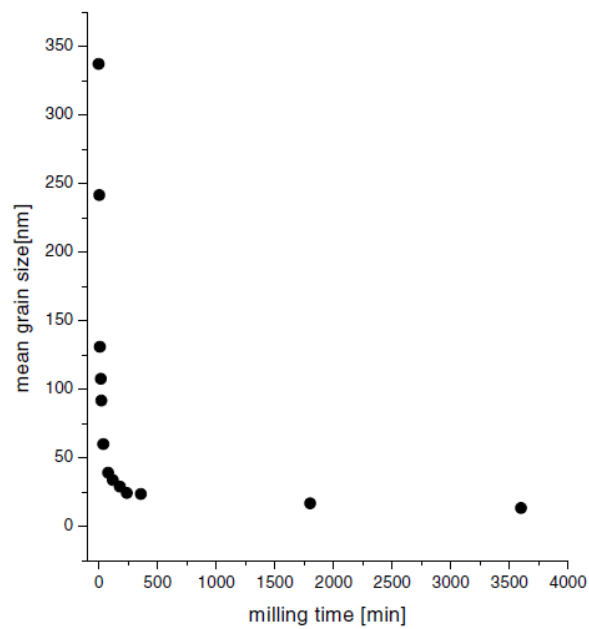


Figure 8: Grain size of corundum vs. milling time [16]

3. Experimental Procedures

3.1 Sample Preparation

The alumina used in this work was received from Sigma-Aldrich. It is 99.5% pure with an average particle size equal to or smaller than 10 μm . The boron used was from SB Boron Corporation. It has an average particle size of 0.7 μm , is amorphous, and has a purity of 95%.

The samples were prepared using a spreadsheet to calculate the mass of each component needed to make multiple batches of 1.0 weight percent boron and 0.2 weight percent boron. Four samples each of 1.0 weight percent boron (Samples 1, 2, 3, and 13), 0.2 weight percent boron (Samples 4, 5, 6, and 14), and pure alumina (Samples 9, 10, 11, and 12) were weighed and placed into a ball mill for different periods of time between 0.3 and 12 hours. A fifth sample of 1.0 weight percent boron (Sample 15) was also made and hand mixed rather than milled. Samples of pure alumina and pure boron (Samples 7 and 8, respectively) were also looked at without any preparation done to them (i.e. the as-received condition). Table 1 lists the original samples batched.

Sample	wt% Boron	Milling Time (hours)	Actual Weight		
			Al ₂ O ₃ (grams)	Boron (grams)	Total (grams)
1	1.0	12	1.9800	0.0200	2.0000
2	1.0	6	1.9801	0.0201	2.0002
3	1.0	3	1.9803	0.0202	2.0005
4	0.2	12	1.9963	0.0044	2.0007
5	0.2	6	1.9964	0.0046	2.0010
6	0.2	3	1.9959	0.0041	2.0000
7	0	0	Pure Alumina as-received		
8	100	0	Pure Boron as-received		
9	0	12	Pure Alumina ~2 grams		
10	0	6			
11	0	3			
12	0	0.3			
13	1	0.3	1.9799	0.0199	1.9998
14	0.2	0.3	1.9972	0.0040	2.0012
15	1	N/A	1.9797	0.0206	2.0003

Table 1: Table of original samples. Sample 15 was hand mixed

3.1.1 Ball Milling

The ball mill used was a Spex Sample Prep 8000M Mixer/Mill with a modified chip allowing the mill to be run for hours as opposed to minutes. Alumina vials and alumina milling balls were used in an effort to eliminate a majority of contamination during the milling process. A single alumina ball with a diameter of 1.27 cm was used as the milling media. The vials can accommodate volumes of 3 to 10 cm³. With the milling media requiring 8.6 cm³, about two grams of powder was used to keep the volume under 10 cm³.

3.1.2 Sintering

One pellet from each powder sample in Table 1 was made using a 0.5 inch diameter powder compaction die pressed to roughly 3500 pounds. Figure 9 shows the Carver Hydraulic Unit Model #3912 press that was used. The die that was used is pictured in Figure 10. The die has an inner diameter of 0.5 inches. The samples were dry pressed without any binders. After the pellets were pressed, they were sintered at 1200°C for 60 minutes in air, while four more samples were left in for an additional 9 hours. The furnace was ramped up at a rate of 30°C/min. All samples were placed on an Al₂O₃ tray during sintering to again try to eliminate contamination. The furnace used was a Thermolyne High Temperature Furnace Model 46200 as pictured in Figure 11.



Figure 9: Press used to create pellets for sintering



Figure 10: Die used to create pellets, disassembled. The inner diameter of the chamber was 0.500”



Figure 11: Furnace used to sinter pellets

Pellets made from all 15 samples from the listed in Table 1 were placed into a furnace to be sintered for one hour. Four additional samples were left in the furnace to be sintered for a total of ten hours. Table 2 summarizes the samples that were pressed into pellets and sintered. The high end of each variable was selected to be analyzed after sintering was finished.

Sample	Static Variable	wt% Boron	Milling Time (hrs)	Sinter Time (hrs)
16	1 wt%B	1	6	1
17		1	3	
18		1	0.3	
19		1	N/A	
20	12 hr milling time	0	12	1
21		1	12	
22		0.2	12	
23	10 hr sinter time	0	0	10
24		0	12	
25		1	12	
26		0.2	12	

Table 2: The samples selected for further analysis after sintering

3.2 Characterization Techniques

3.2.1 X-ray Diffraction (XRD)

X-ray diffractometry is typically used to identify the crystal structure and phases of a crystalline material. X-rays are incident upon a material and the beam interacts with the sample. A part of the beam is reflected as a diffracted beam. Bragg's law explains the way these diffracted beams interact with each other. Bragg's law is written as:

$$n\lambda = 2d_{hkl}\sin\theta \quad (\text{Eq. 2})$$

In Bragg's law, λ is the wavelength of the x-rays, n is the integer number order of diffraction, d is the interplanar spacing in the crystal, hkl are the Miller plane indices, and θ is Bragg's angle. The XRD used in this work was a Bruker D8 Discover with a copper x-ray source with a wavelength of 1.54049 Å. The powder samples were placed

directly into a packed powder sample holder in the machine. The sintered pellets were placed on a clay holder instead of a packed powder holder. Scans were made from 10 to 90 degrees 2-theta using a scan rate of 0.3 seconds per step for a total of 3944 steps. Each scan took roughly 20 minutes to complete. Samples were not rotated during the test. XRD was done on each sample in this work.

The average crystallite size, in angstroms, can also be calculated by using the Scherrer Equation. Using the peak with a 2-theta equal to 35.15° , the crystallite size was hand calculated for Samples 1 and 9 to compare to the other sources of crystallite size. Samples 1 and 9 are 1.0 weight percent boron and pure alumina, respectively, which have been milled for 12 hours.

3.2.2 Scanning Electron Microscope (SEM)

Scanning electron microscopy can be used to provide topographical information about coatings or powders. By doing SEM on the powder, it can show the size and shape of the powder before and after the sintering process. The SEM used in this work was a TopCon SM-300 with operating voltages from 10 to 20 kV. Each of the samples analyzed in the SEM were sputter coated with an Au-Pd coating to enhance the conductivity. All samples from Table 1 and Table 2 were observed at magnifications between 200 and 2000x.

3.2.3 Porosity

Porosity of the post-sintered pellets was measured using the Archimedes method of porosity. Each pellet was weighed dry. The pellets were then dropped into water, brought to a boil, left at a boil for a few minutes, and allowed to cool back to room temperature while remaining in water. Two additional measurements were made at this point. The first weight recorded was the mass of the pellet in a basket suspended in water from the bottom of the balance and the second was made using the water-saturated sample in air after removing all beads of water on the surface.

The porosity of the sintered pellets was calculated using this equation:

$$Porosity \% = \frac{m_s - m_d}{m_s - m_{ss}} \times 100\% \quad (\text{Eq. 3})$$

where m_s is the mass of the pellet when saturated with water in air, m_{ss} is the mass of the pellet saturated with water while suspended in water, and m_d is the mass of the pellet when dry before any water saturation. Figure 12 shows the setup of the balance that was used to obtain the results. A Mettler Toledo Model MS304S balance with a 0.1mg resolution was used to take mass measurements.

Figure 13 shows the sintered pellets. The unmilled pellets had a difficult time holding together after sintering indicating poor sintering. Sample 23 (pure alumina in the as-received condition) is the only pellet that did not hold together enough to make accurate measurements.



Figure 12: (Left) Scale setup used to make weight measurements for porosity (Right) Basket used to suspend pellets in second weight measurement

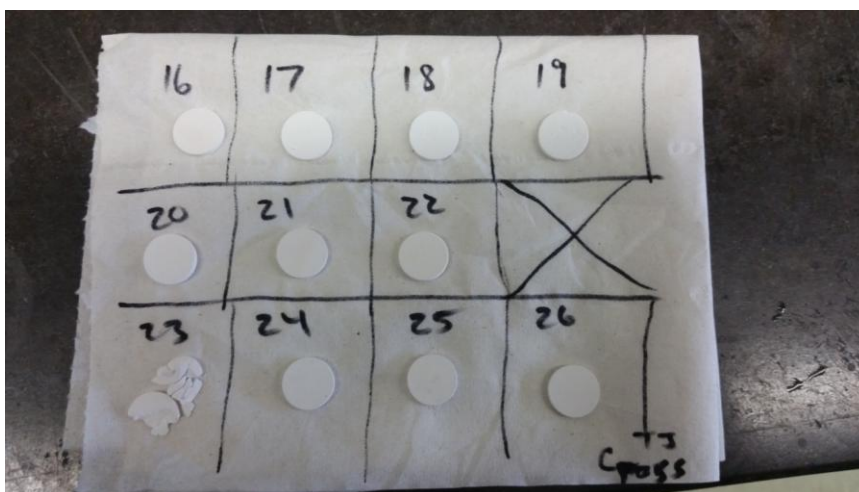


Figure 13: The samples selected to be analyzed after sintering

4. Experimental Results and Discussion

4.1 XRD

A corundum standard was run each day before any samples were run to ensure the machine was in working order. Samples were analyzed using the Bruker analysis software, Diffrac.Suite. This analysis program pulls files from the Crystallography Open Database (COD) and provides multiple matches to the diffraction pattern. Figure 14 shows a standard XRD pattern obtained from a sample with 0.2 weight percent boron. The major phase present was found to be corundum (file number COD1000032, as shown in Figure 14) with no apparent secondary phases.

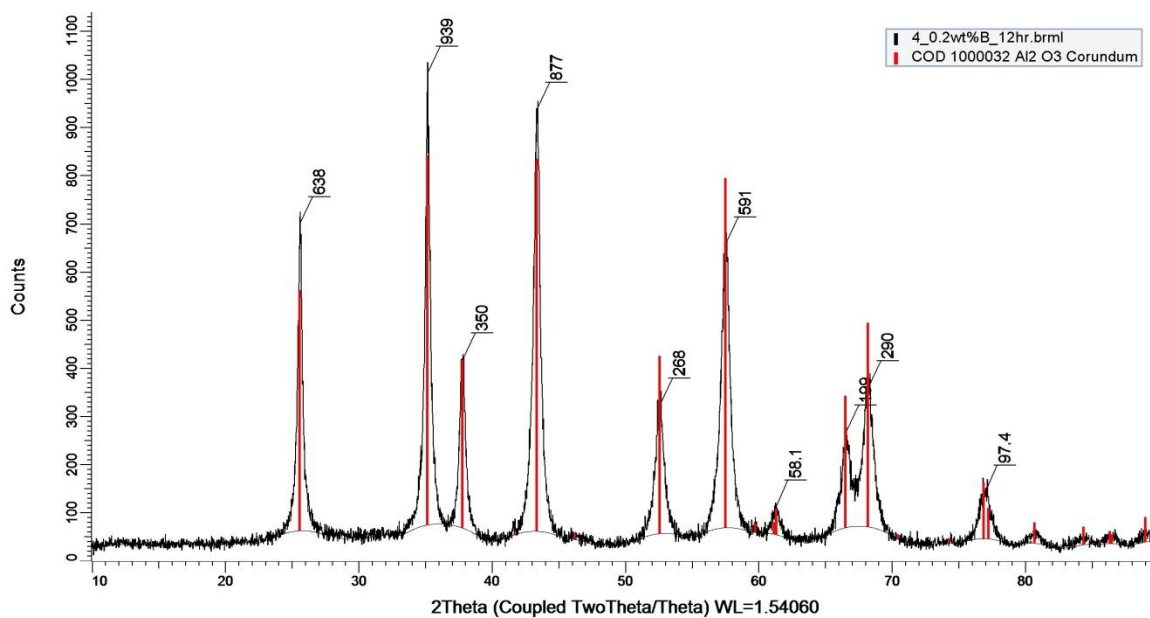


Figure 14: XRD pattern of sample of 0.2 wt% boron

Figures 15 and 16 show the effects of ball milling on samples with 1.0 weight percent boron added. It is clear that the peak width increases with increased milling time. The increase in peak width correlates to a decrease in crystallite size as milling time increases. There are two peaks in the sample that was hand mixed and the sample that was only milled for 0.3 hours that disappear after being milled for a longer period of time. These peaks are likely coming from a β -phase of alumina.

The effects of sintering on samples of 0.2 weight percent boron are shown in Figures 17 and 18. Looking at these diffraction patterns, it is clear that this small amount of boron has very little effect, if any at all, on the sample. If this small amount of boron does affect the results, the additional aluminum borate phase is too small to detect. It is likely that larger amounts of boron would need to be added to see any difference in the diffraction patterns.

Figure 19 and 20 show the effects of sintering of samples of 1.0 weight percent boron when they are milled for 12 hours. Additional peaks appear after sintering for 1 hour, but then disappear when left in the furnace for 10 hours. These additional peaks are marked with a triangle or square (alumina and aluminum borate, respectively) to clearly indicate which peak comes from which phase. The disappearing of these peaks could be due to two things happening: one being the boron evaporating during the extended period of sintering, while the other would be where the boron absorbs into the alumina. The first is highly unlikely due to the boiling point of boron being over 2000°C and the sample was sintered only in a 1200°C furnace in air. The second would cause shifts in the peaks of alumina. There is no visible shift in the alumina, if any at all, so this likely not the cause of the peaks disappearing either.

Figure 21 and 22 show the diffraction patterns of samples that have been milled for 12 hours and sintered for 1 hour as boron composition increases. Again, the peaks with two phases are marked with a triangle or square to specify which peaks are from which phase. Following the pattern before, the diffraction patterns of pure alumina and 0.2 weight percent boron are quite similar, reinforcing that 0.2 weight percent boron has little to no effect on the diffraction patterns.

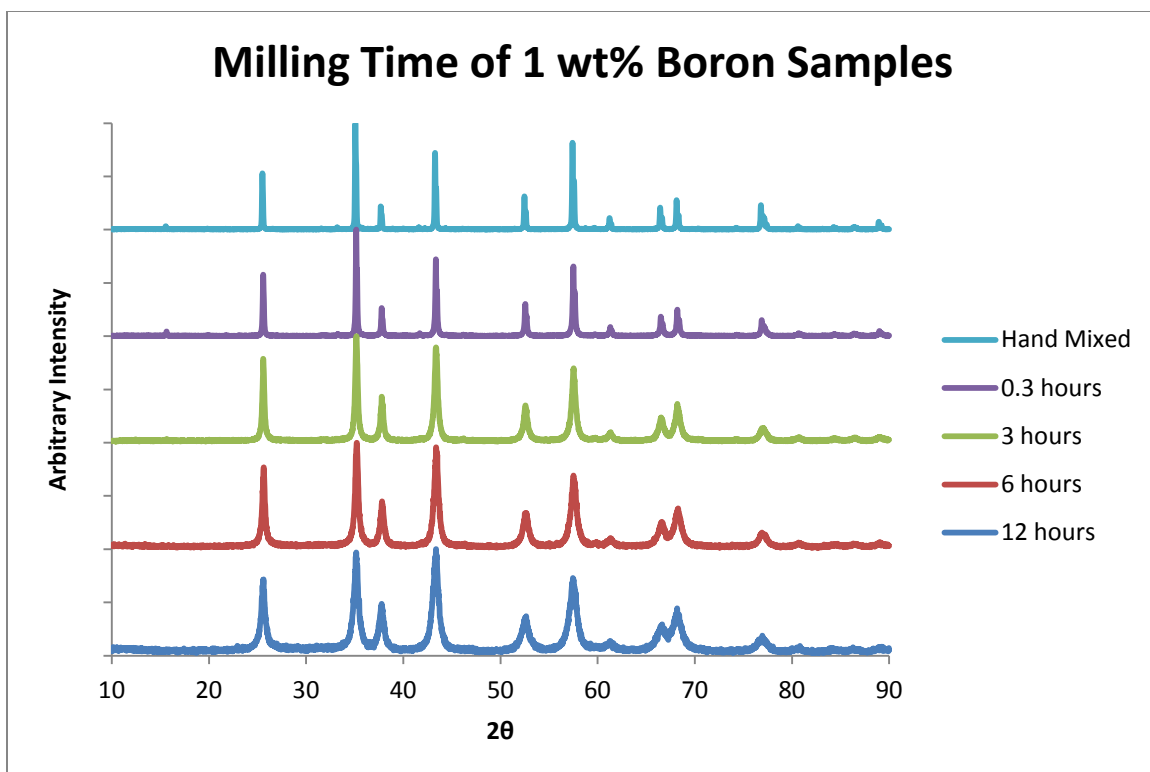


Figure 15: 1.0 wt% boron before sintering

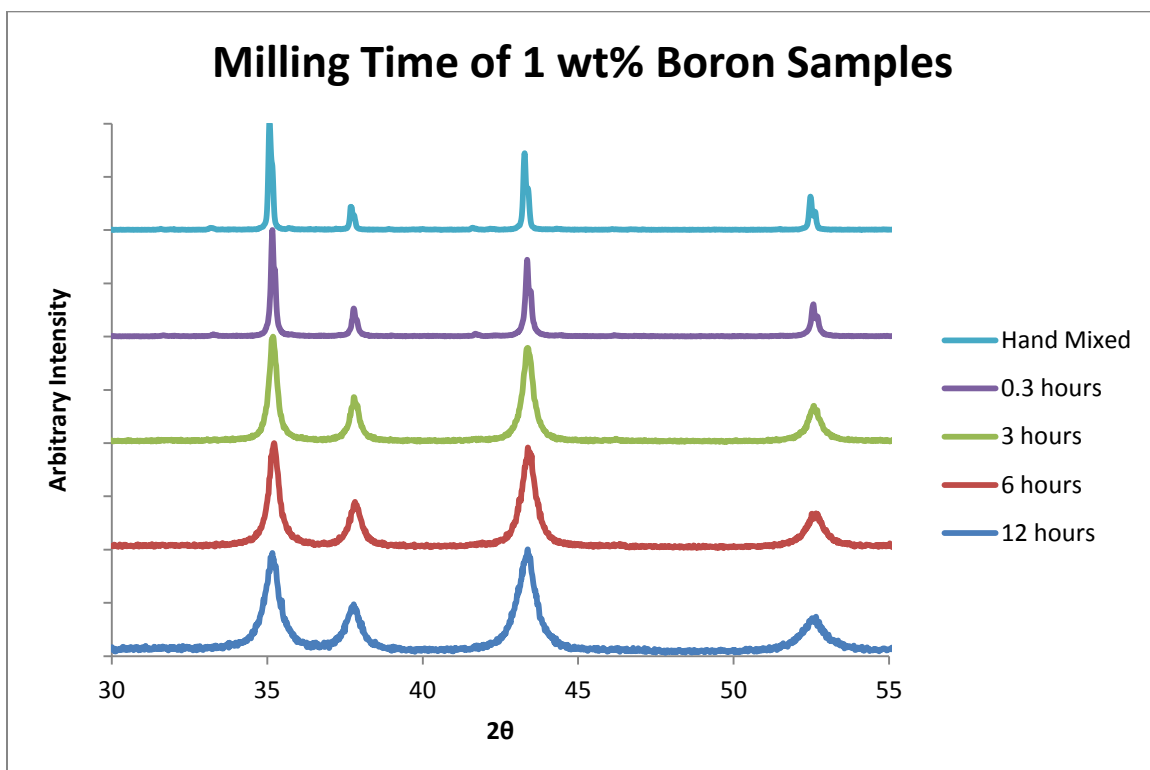


Figure 16: 1.0 wt% boron before sintering from 30° to 55° 2θ

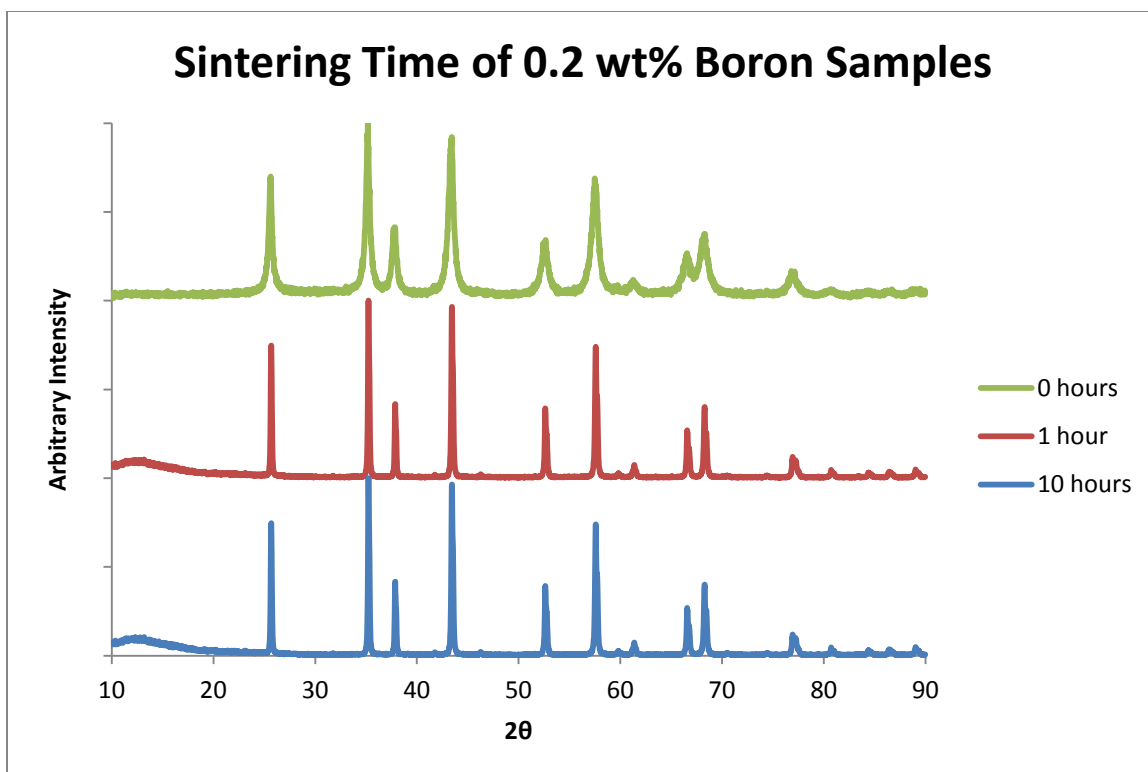


Figure 17: 0.2 wt% boron milled for 12 hours

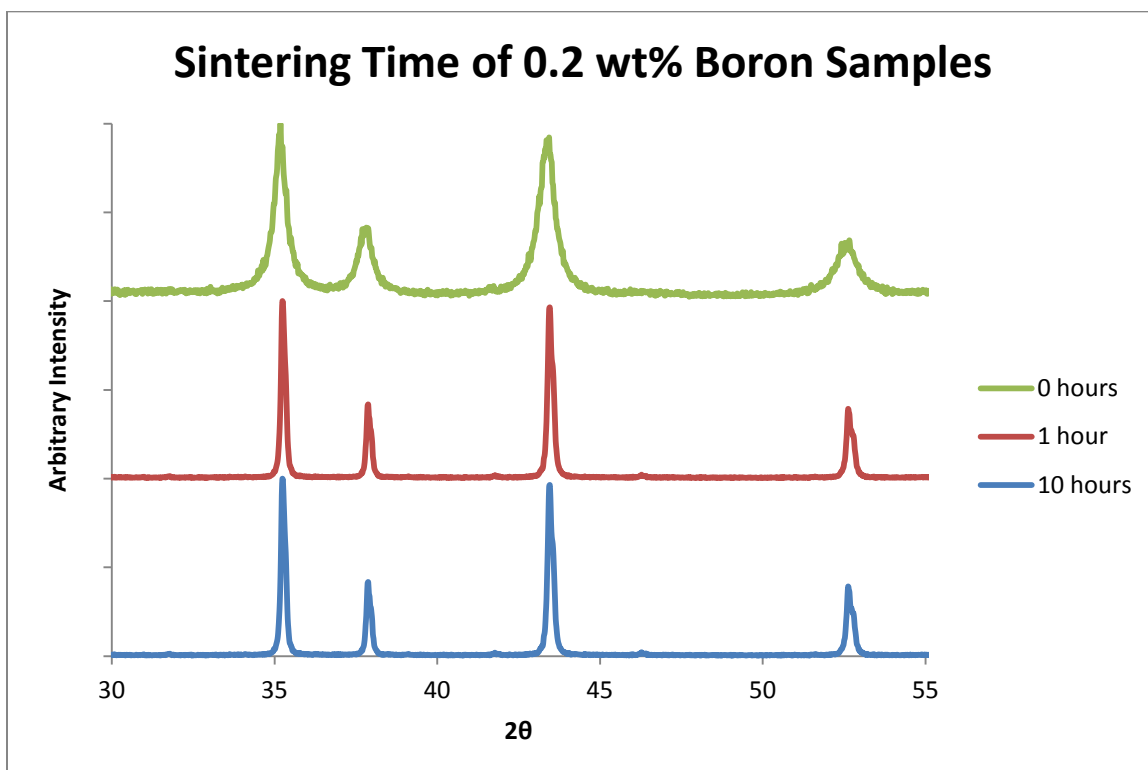


Figure 18: 0.2 wt% boron milled for 12 hours from 30° to 55° 2θ

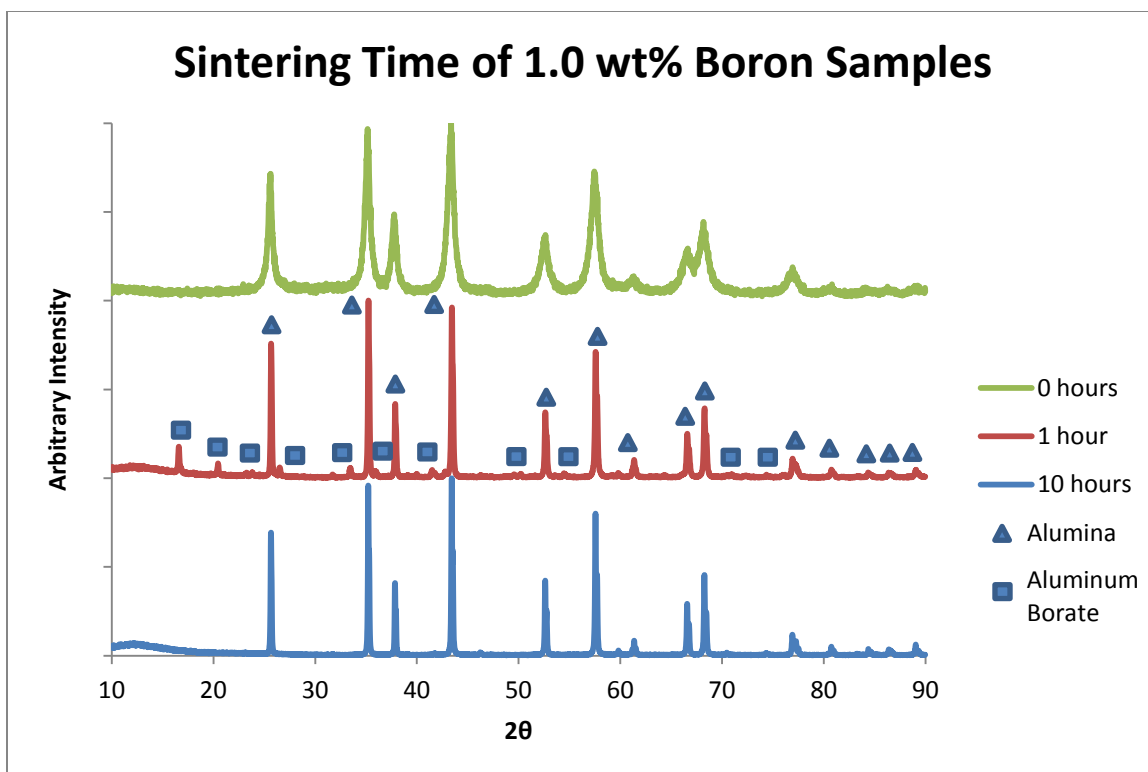


Figure 19: 1.0 wt% boron milled for 12 hours

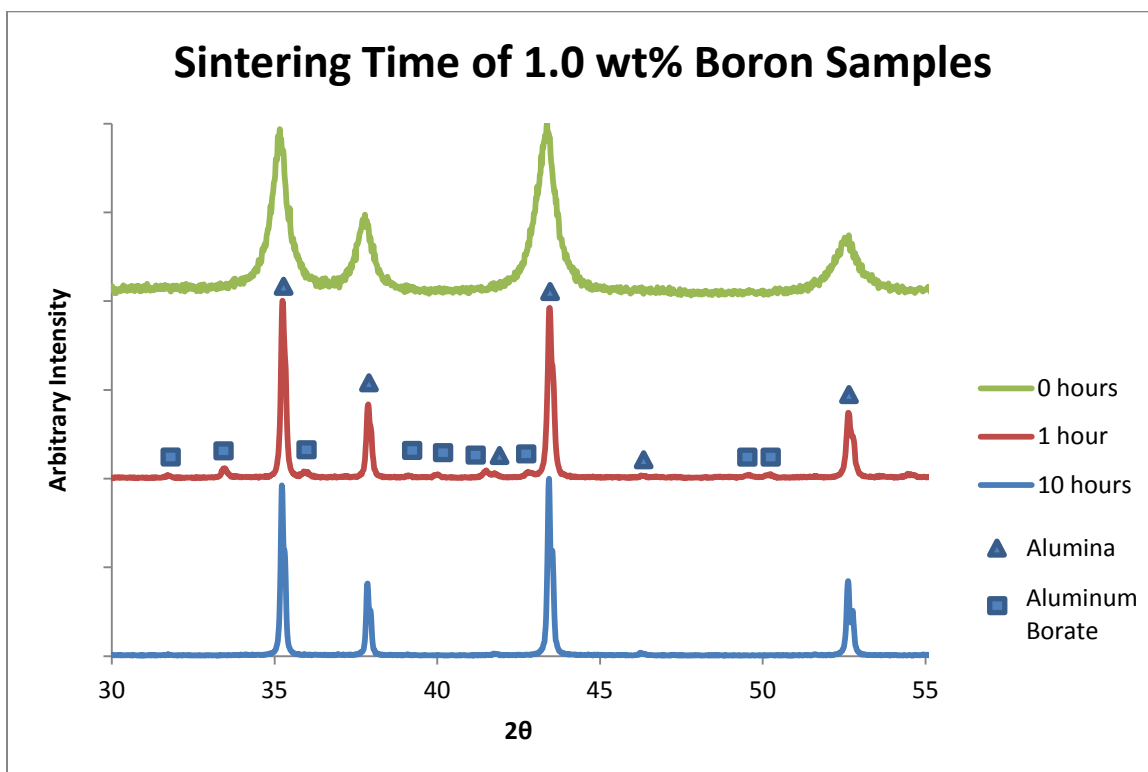


Figure 20: 1.0 wt% boron milled for 12 hours from 30° to 55° 2θ

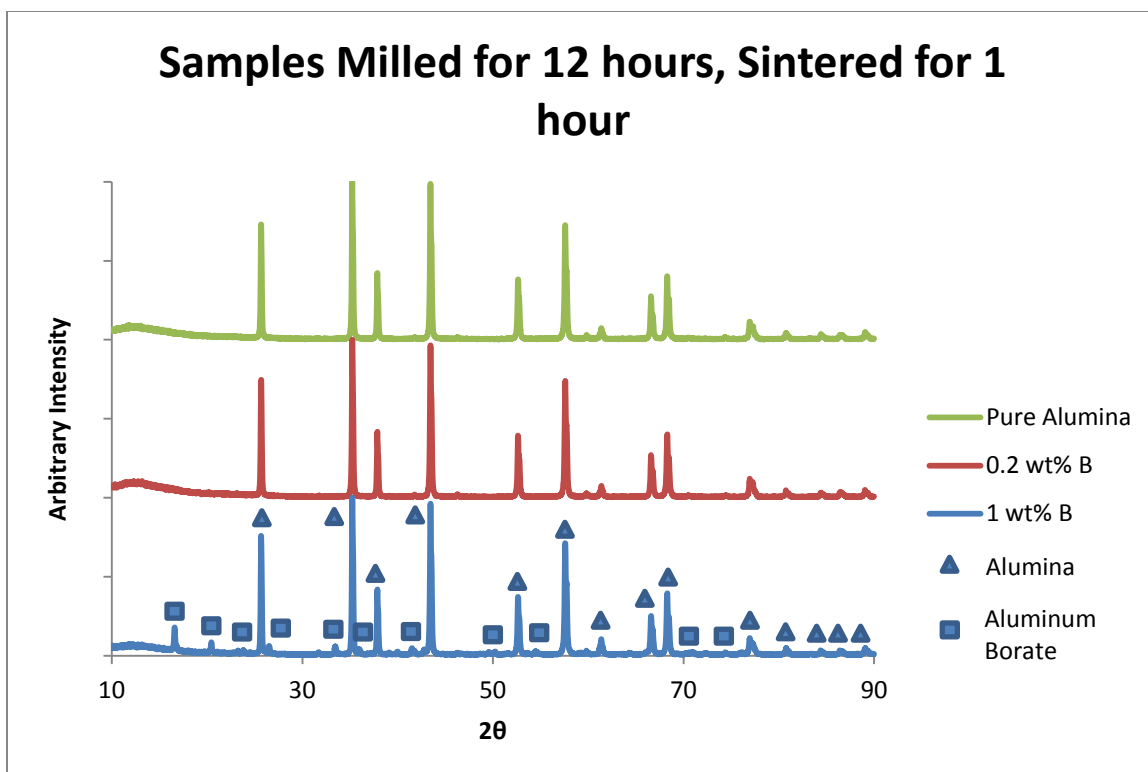


Figure 21: Samples milled for 12 hours, sintered for 1 hour

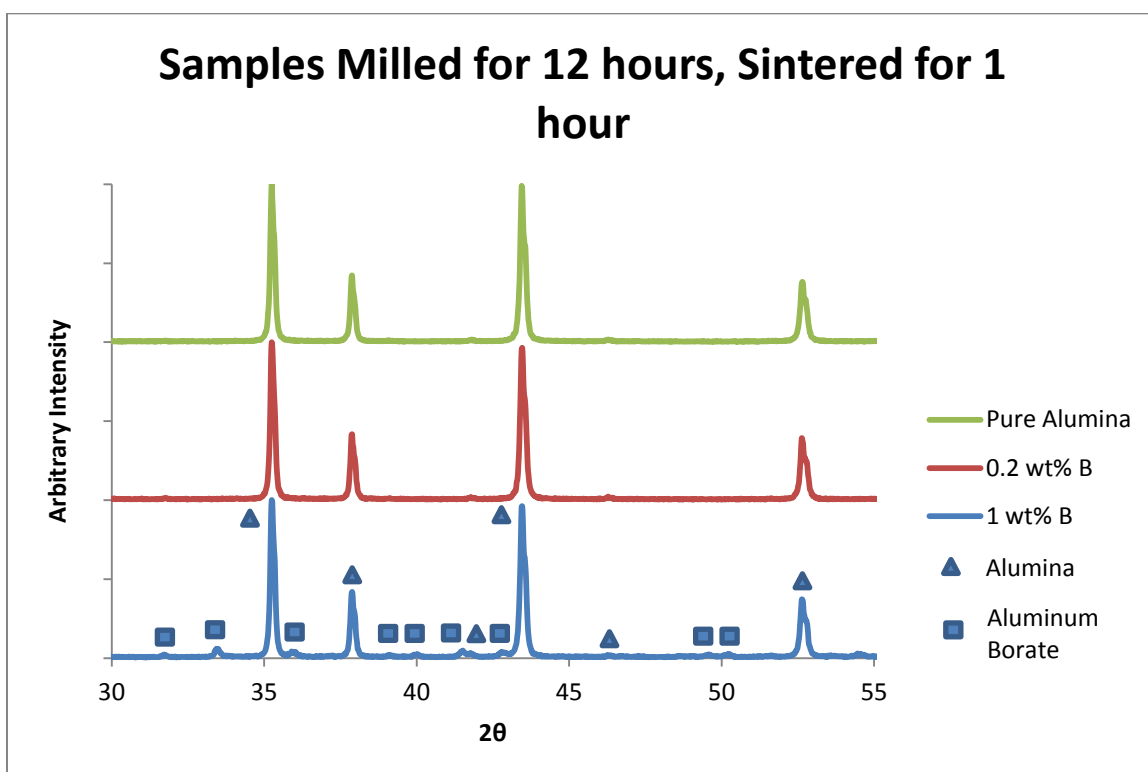


Figure 22: Samples milled for 12 hours, sintered for 1 hour from 30° to 55° 2θ

Figure 23 shows crystal properties of powder samples 1 through 15 from Table 1 as the amount of time spent in the ball mill increases. Crystallite size steadily decreases as milling time increases as Figure 23 (a) shows. According to this trend, milling much past 12 hours would prove to be wasteful due to the decrease in crystallite size leveling off between 10 and 12 hours. The changes in the lattice parameters as a function of milling time are shown in Figures 23 (b) and (c). There is not a clear trend on what happens to either lattice parameter as milling time increases. Lattice parameters are much more difficult to measure precisely than crystallite size, which could cause the randomness of the lattice parameters while still maintaining crystallite size accuracy.

Crystallite size was also determined by using a data analysis software developed by Luca Lutterotti called Materials Analysis Using Diffraction, otherwise known as MAUD [17]. MAUD allows the uploading of data files and phases from database files and analyzes them based on the Rietveld method. The Rietveld method uses a non-linear least squares algorithm in order to reduce the residual function. There are many pros using this method such as using the measured intensity points directly and it uses the entire spectrum. The cons of the Rietveld method are that it requires a model and it needs a wide spectrum [18]. The phase files used for this part of this work were obtained from the Crystallography Open Database (COD), which is the same database that the Bruker XRD software uses. The files from used from the COD were COD1000032 for the corundum phase and COD9005085 for the aluminum borate phase. When doing crystallite calculations, the crystallite size of only the alumina phase was used. MAUD also calculates the lattice parameters of the material. Figures 24 and 25 contain the calculated crystallite sizes from both the MAUD program and the Bruker software.

Figure 24 shows the crystal properties of the 1.0 weight percent boron samples as milling time increases after sintering for one hour. As seen in Figure 24 (a), the Bruker software shows a slight decrease in the post-sintered crystallite size as milling time increases. The MAUD results do not show a strong trend. Figures 24 (b) and (c) show the lattice parameters after sintering; only the lattice parameters calculated from MAUD were used. Figure 24 (b) roughly shows an increase in lattice parameter (a) as time increases and a plateau at 6 hours of milling. Lattice parameter (c) is shown to have the same trend in Figure 24 (c). A better idea of these trends could be observed with a larger sample size. For example, samples milled for two, five, and nine hours would fill some of the gaps.

Figure 25 shows the samples that were milled for 12 hours and then sintered for one hour and 10 hours as the weight percentage of boron increases. The crystallite size trends in both MAUD and Bruker results are relatively similar. There are no sharp increases or decreases in crystallite size for the samples sintered for one hour. The samples that were sintered for 10 hours follow a different trend than the samples sintered for one hour. Again the two trends are quite similar between the MAUD and Bruker results. Both samples seem to have a sharp decrease followed by a plateau between 0.2 and 1.0 weight percent. For the lattice parameters in Figures 25 (b) and (c) only MAUD was used to obtain the results. Both lattice parameters for the samples sintered for one hour stay very close to the same regardless of boron composition as shown in Figures 25 (b) and (c). The lattice parameters of the samples that were sintered for 10 hours, however, follow a different trend. Again, it is a sharp decrease followed by a plateau or a very slight increase.

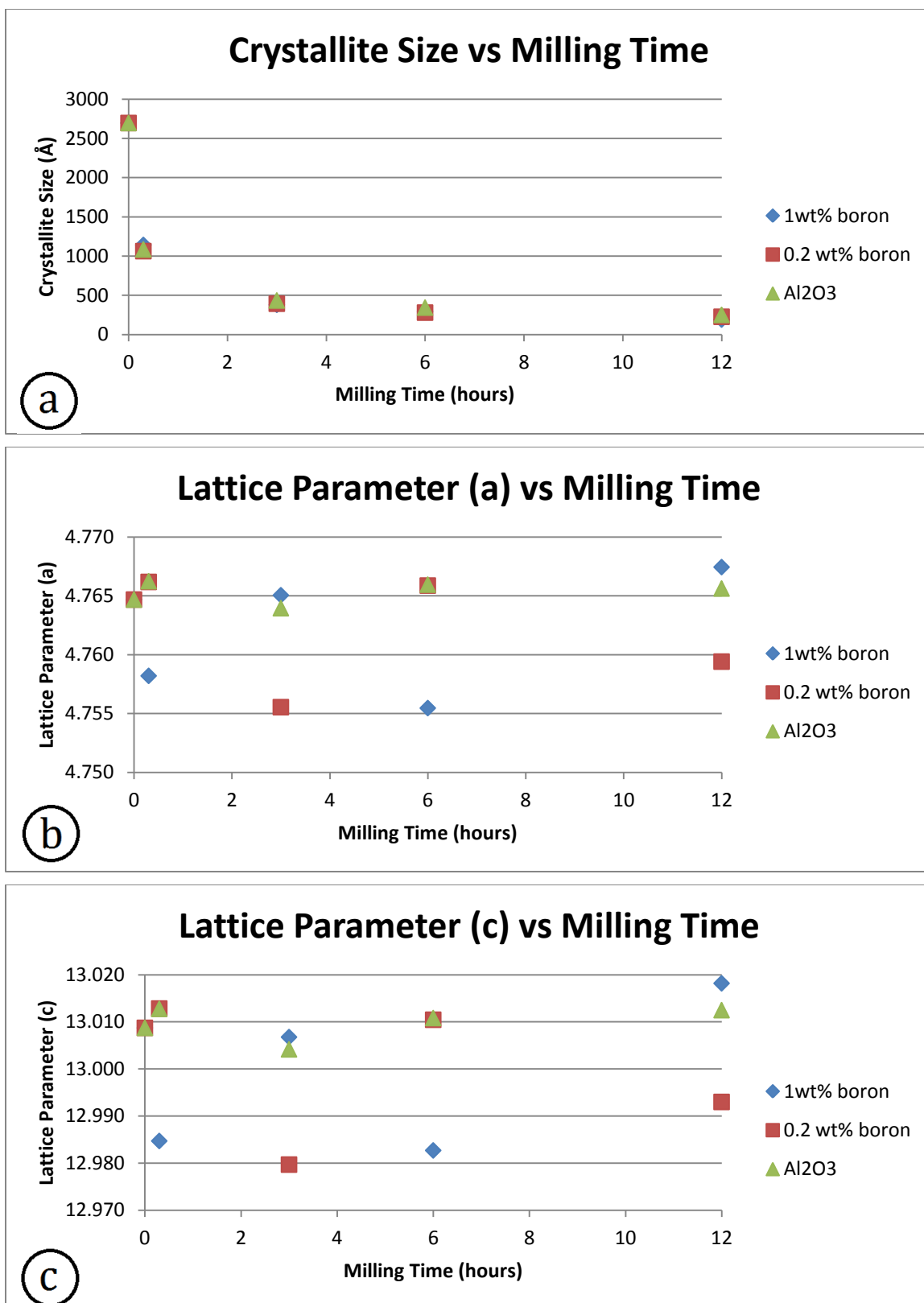


Figure 23: Crystal properties vs. milling time – Before sintering

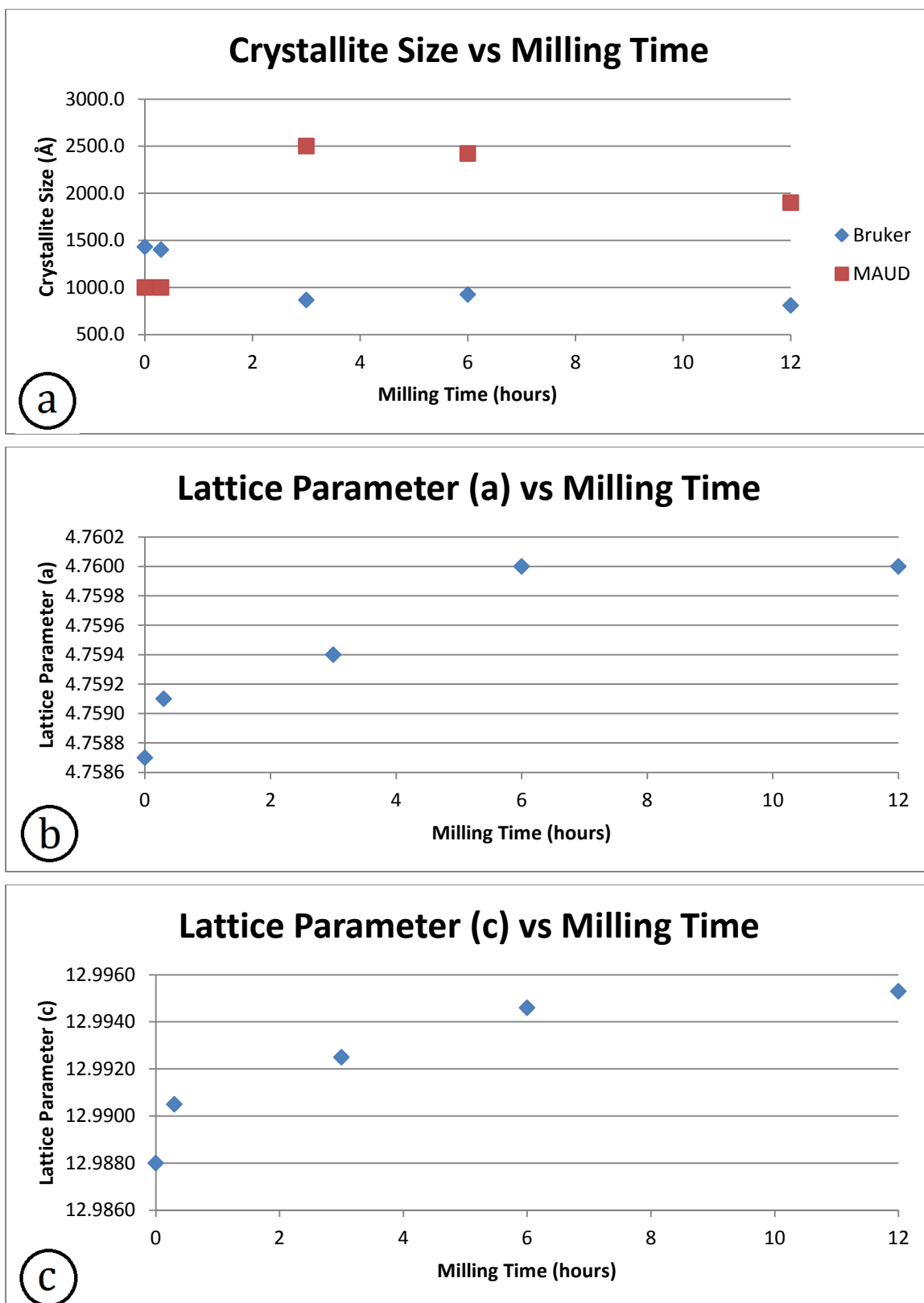


Figure 24: Crystal properties vs. milling time of 1.0 wt% boron samples – After sintering

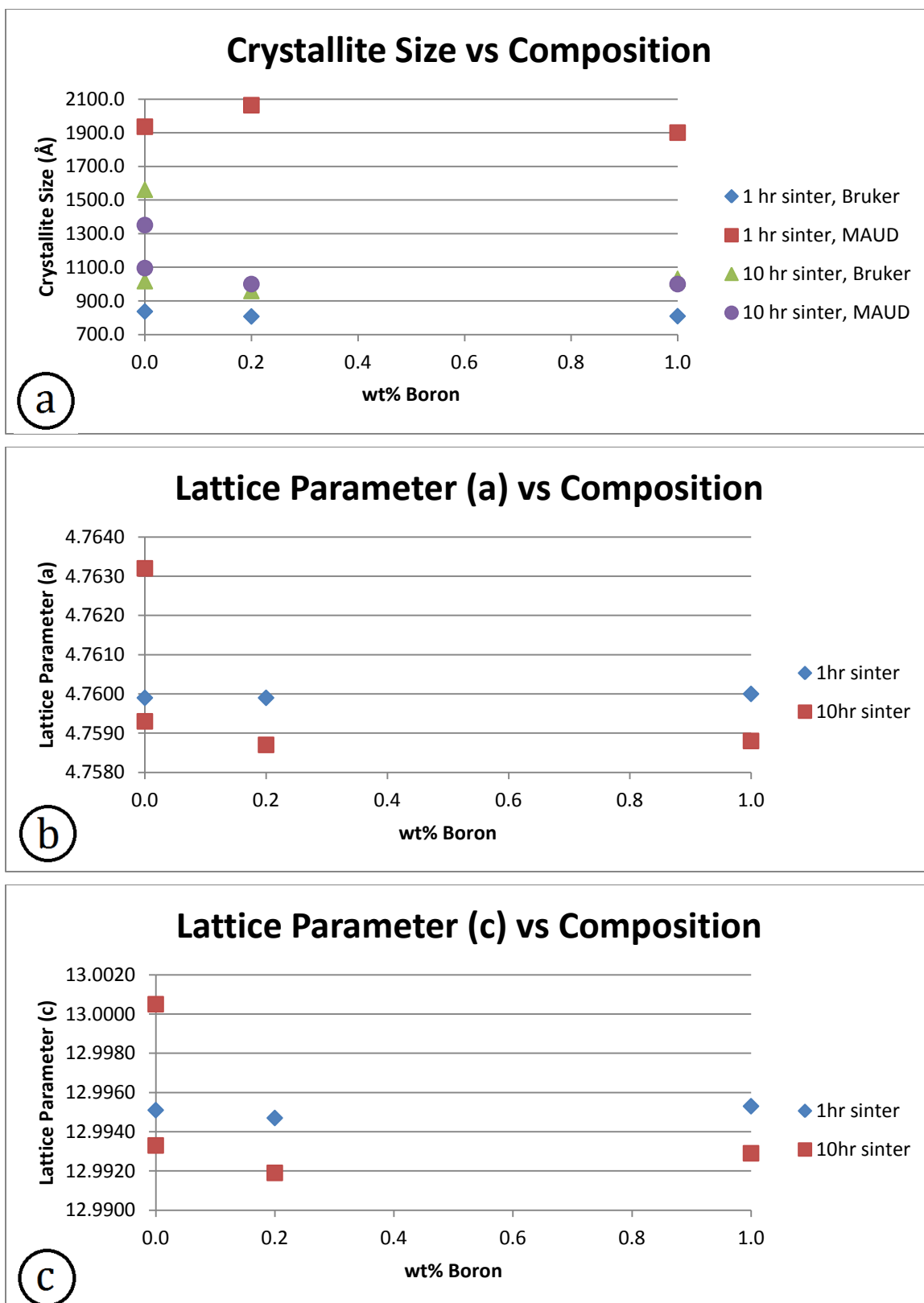


Figure 25: Crystal properties vs. composition of 12-hour milled samples – After sintering

The crystallite size of samples 1 and 9 was calculated using the Scherrer equation (Eq. 1) to see how it compared to the MAUD and Bruker results. The peak at 35.15 degrees 2-theta was used for each sample.

Table 3 compares the three different means of calculating the crystallite size. The three methods used were MAUD, the Bruker XRD Analysis software, and the Scherrer Equation. This shows that MAUD is less reliable for the crystallite size as most of the samples came back at 1000 Å. The Scherrer equation could be used as a rough estimate for the sample's average crystallite size. The Bruker software is likely the least error prone source of calculating the crystal size. There are too many possible sources of error in the other two methods such as programming errors in MAUD or human errors using the Scherrer Equation.

Sample #	wt% Boron	Milling Time	Sintering Time	MAUD Crystallite Size (Å)	Bruker Crystallite Size (Å)	Scherrer Crystallite Size (Å)
1	1	12	0	191	165	125
9	0	12	0	250	216	182
16	1	6	1	2423	925	N/A
17	1	3	1	2502	867	N/A
18	1	0.3	1	1000	1402	N/A
19	1	N/A	1	1000	1431	N/A
20	0	12	1	1936	837	N/A
21	1	12	1	1901	809	N/A
22	0.2	12	1	2064	808	N/A
23	0	0	10	1095	1561	N/A
24	0	12	10	1351	1018	N/A
25	1	12	10	1000	1031	N/A
26	0.2	12	10	1000	959	N/A

Table 3: Calculated crystallite size from various sources. Sample 19 was hand mixed

4.2 SEM

The as-received alumina and boron powders were observed in the SEM before any processing was done to them. These samples are shown in Figure 26 at 200x and 1000x magnification. All samples in this work were sputter coated with an Au-Pd coating to reduce charging effects encountered with non-conducting samples.

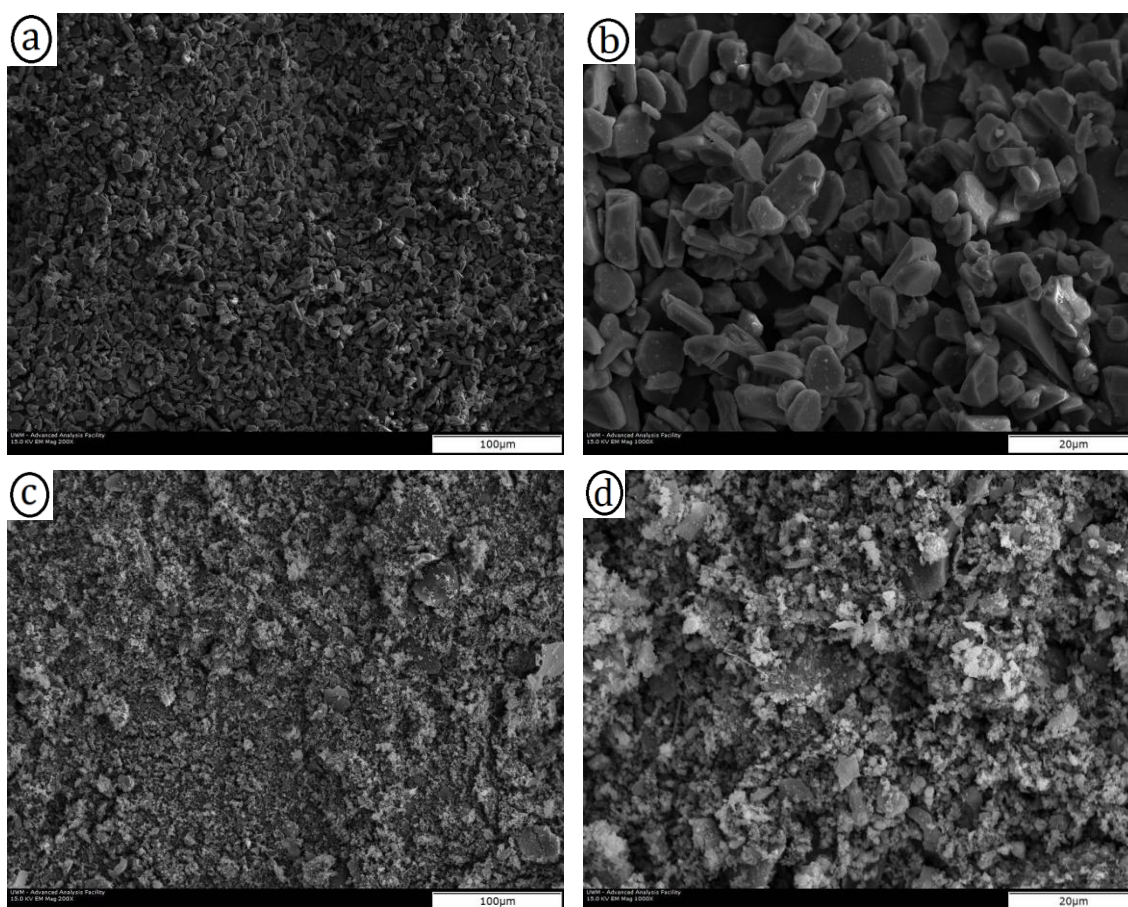


**Figure 26: Components as-received at 200x and 1000x magnification
(a) Alumina at 200x, (b) Alumina at 1000x, (c) Boron at 200x, (d) Boron at 1000x**

Figure 27 shows how the samples looked after being milled for various amounts of time. As milling time increases, it is clear to see that the samples are becoming mixed much better than at the lower milling times.

Figure 27 (a) is the 1.0 weight percent boron sample that was hand mixed instead of ball milled. This looks almost identical to Figure 26 (a), which is solely alumina before any milling has occurred. The hand mixed sample is likely to be poorly mixed as the components were placed into a bag and mixed by hand. While appearing mixed to the eye, this would not be expected to form as uniform a mixture as the Spex mill processing.

As the milling time increases to 0.3 hours, it appears that the particles become a marginally smaller in Figure 27 (b). This still looks mostly like the alumina did as prior to any milling.

Figures 27 (c), (d), and (e) show that the sample is clearly better mixed and as the diffraction patterns showed, the particle size is decreasing steadily to nano-scale particles with an increase in milling time. The nano-sized particles are agglomerated together to form larger appearing particles. These samples' topography agrees with the crystallite size versus milling time plots from the Bruker analysis results as shown in Figure 23. All samples in Figure 27 had a uniform topography throughout.

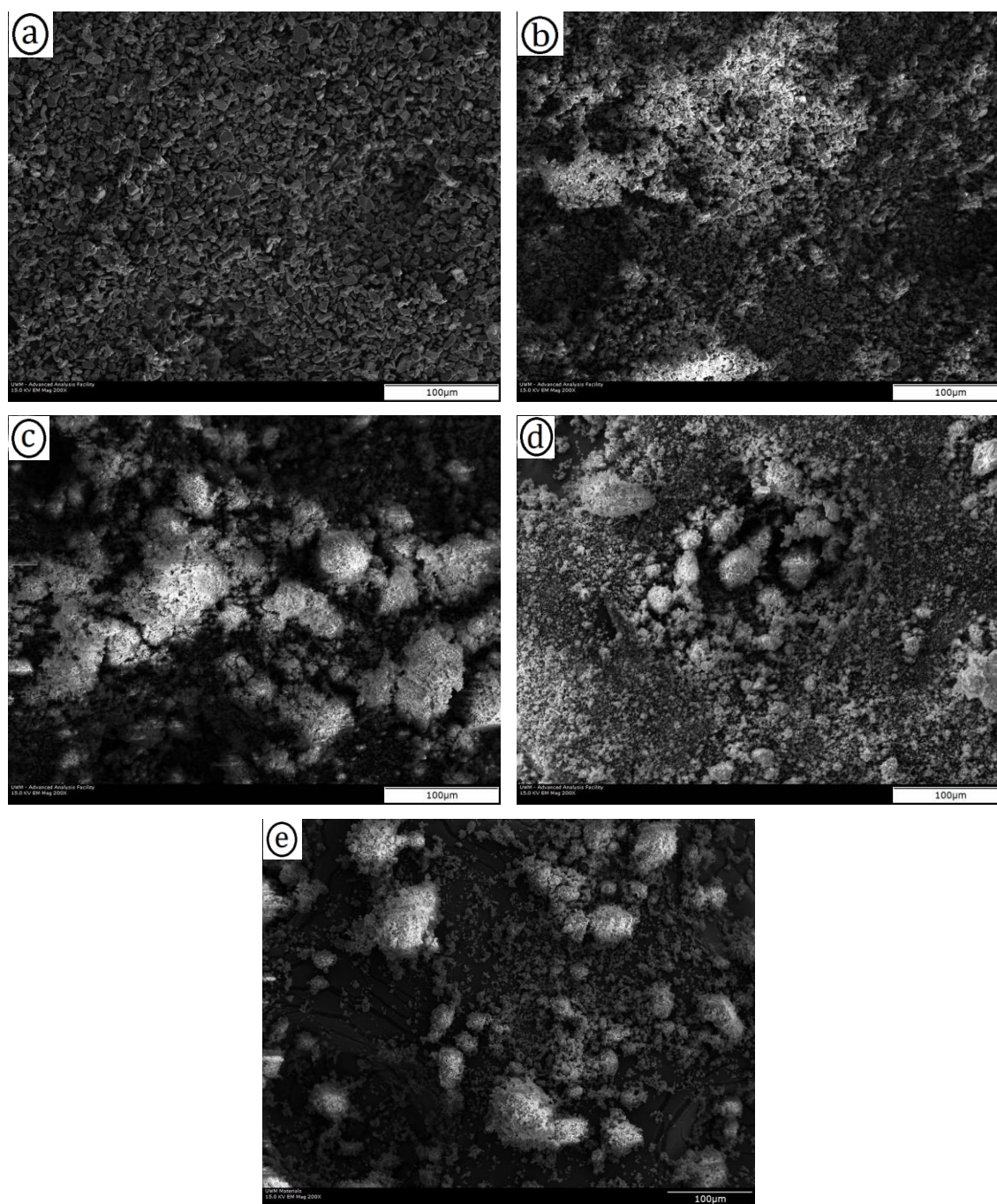
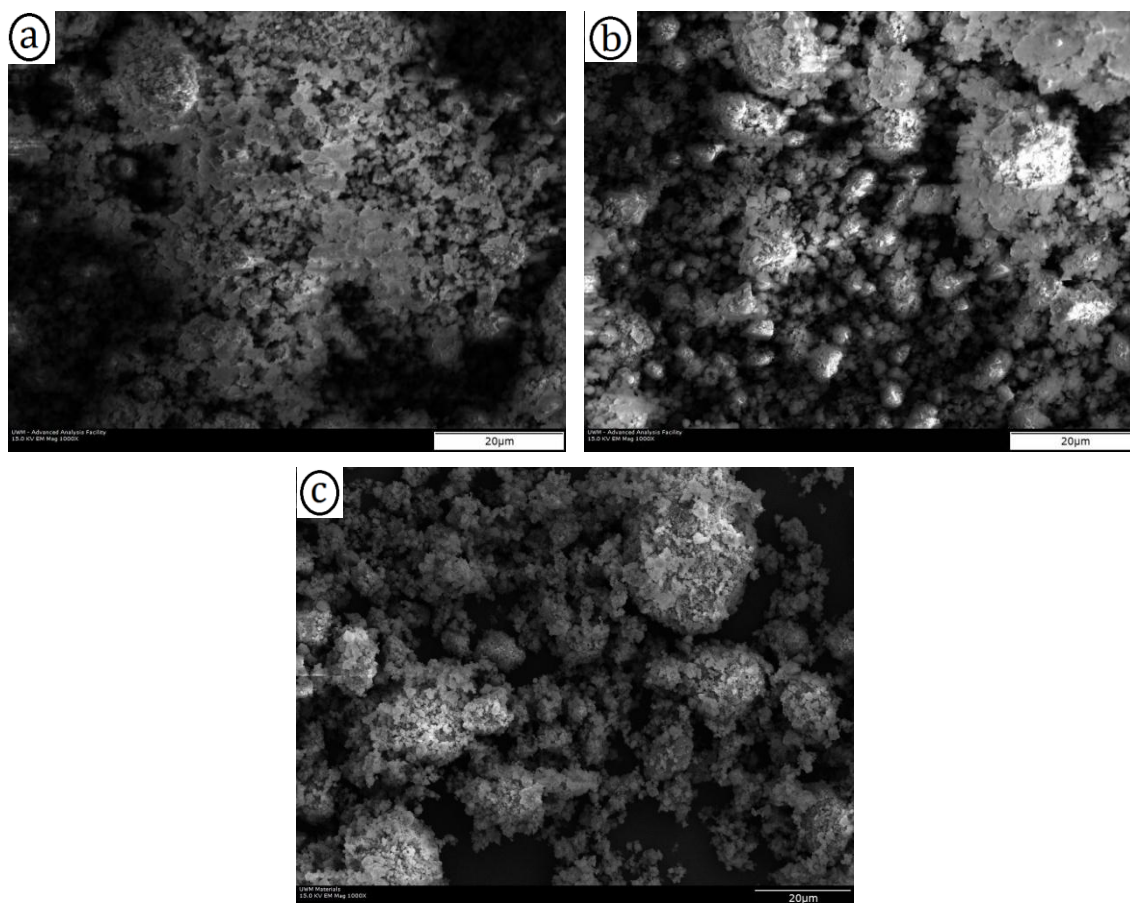


Figure 27: Samples of 1.0 wt% boron milled for various amounts of time at 200x magnification
(a) Hand Mixed, (b) 0.3 hours, (c) 3 hours, (d) 6 hours, (e) 12 hours

Figure 28 shows how the powders appeared as the weight percentage of boron was increased after milling for 12 hours and before sintering. Figure 28 (a) is pure alumina, Figure 28 (b) is 0.2 weight percent boron, and the Figure 28 (c) is the sample with 1.0 weight percent boron. All of these samples show that after milling, large particles are just made of smaller bits of alumina, and boron in (b) and (c), crushed together. All of these samples had a uniform topography throughout.



**Figure 28: Samples milled for 12 hours before sintering at 1000x magnification
(a) Pure Al_2O_3 , (b) 0.2 wt% boron, (c) 1.0 wt% boron**

Figure 29 shows pure alumina milled for 12 hours as sintering time goes up. Figure 29 (a) shows the morphology of pure alumina after being milled for 12 hours before sintering. Large agglomerates are formed and composed of smaller alumina particles. After sintering for one hour, the particles in Figure 29 (b) have been packed together, there is much visible porosity. There is an even further densification shown in Figure 29 (c). The samples in Figure 29 have a uniform topography over the entire surface of the pellet.

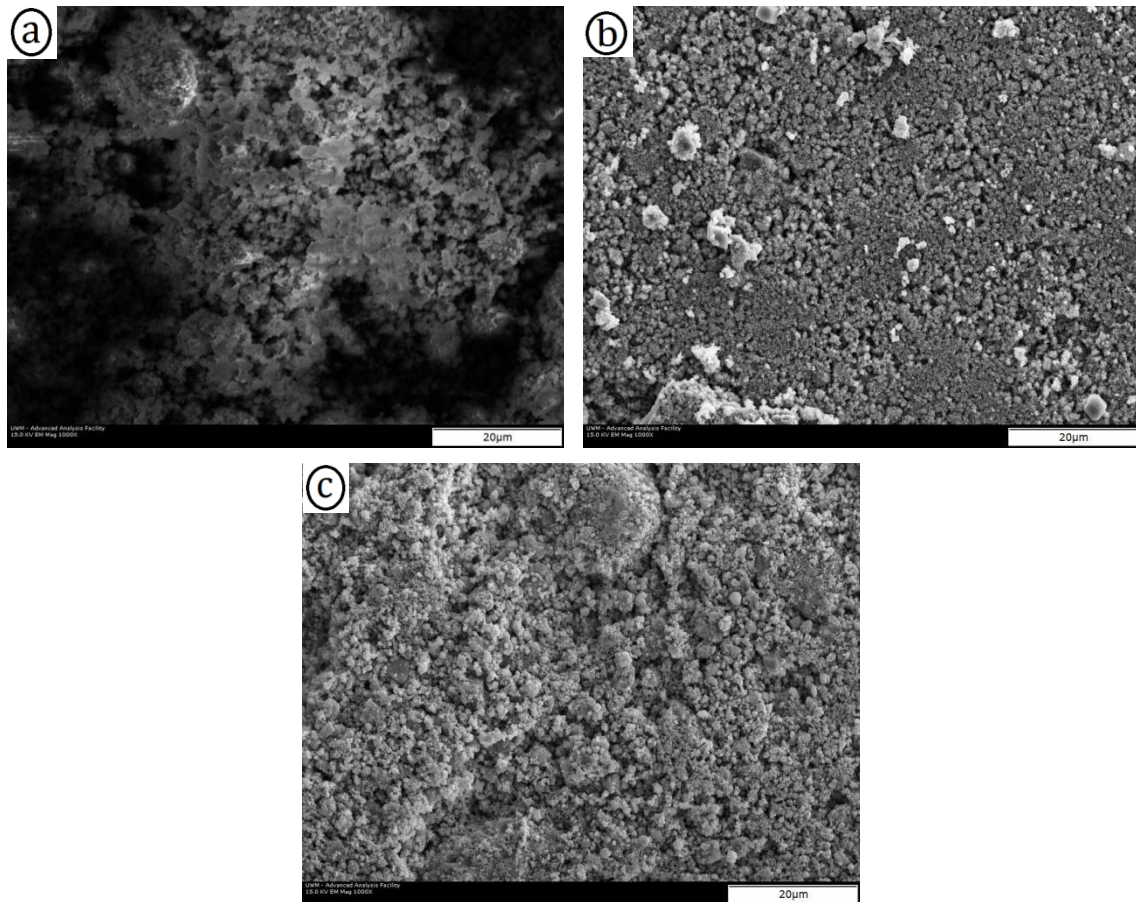
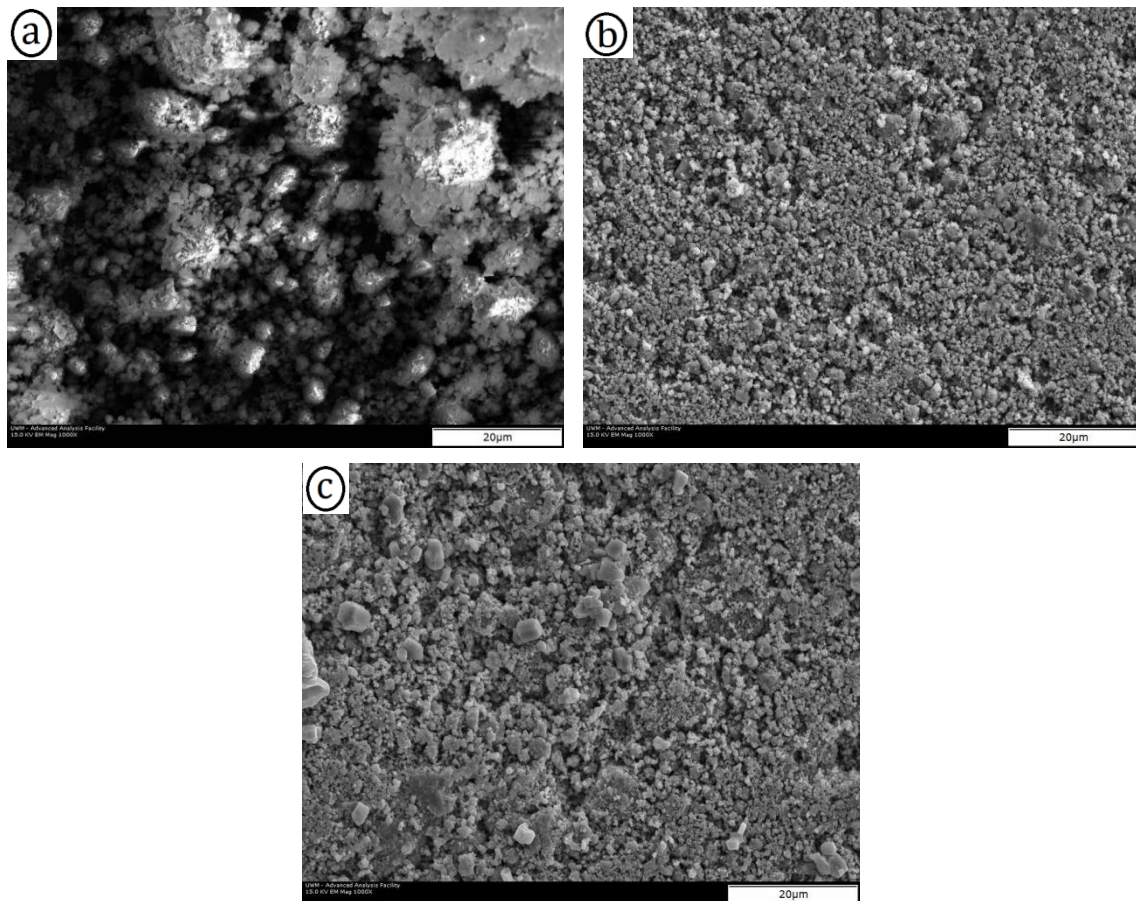


Figure 29: Al₂O₃ milled for 12 hours at 1000x magnification
(a) Before sintering, (b) Sintered for 1 hour, (c) Sintered for 10 hours

Figure 30 shows the samples with 0.2 weight percent boron as sintering time increases. These samples follow the same trend as the samples in Figure 29. There is still a high amount of porosity in both Figures 30 (b) and (c). There are some particles in the sample that was sintered for 10 hours, Figure 30 (c), that are not nano-sized, which is contradictory to the other samples that were milled for 12 hours. All of the samples in Figure 30 have a uniform topography.



**Figure 30: 0.2 wt% Boron Milled for 12 hours at 1000x magnification
(a) Before Sintering, (b) Sintered for 1 hour, (c) Sintered for 10 hours**

The sample of 1.0 weight percent boron that has been milled for 12 hours is shown in Figure 31 at different sintering times. The pre-sintered topography is shown in Figure 31 (a), the alumina and boron particles before sintering are agglomerated together. Again, all of the larger particles are agglomerates composed of smaller particles. Figures 31 (b) and (c) show the pellets that were sintered for one hour. These samples follow the same trend as the samples in Figure 29 as well. All of the samples in Figure 31 have a uniform topography.

The pellet that was sintered for 10 hours in Figure 31 (c) shows an even further densification over that of Figure 31 (b), which is in line for the observed pellet diameter shrinkage that is discussed in the next section.

In all three pictures of Figure 31, it is clear that the samples have been mixed thoroughly as opposed to the mostly unmixed samples in Figures 27 (a) and (b). The topography of these samples reinforces the results from the crystallite size versus plots in the previous section.

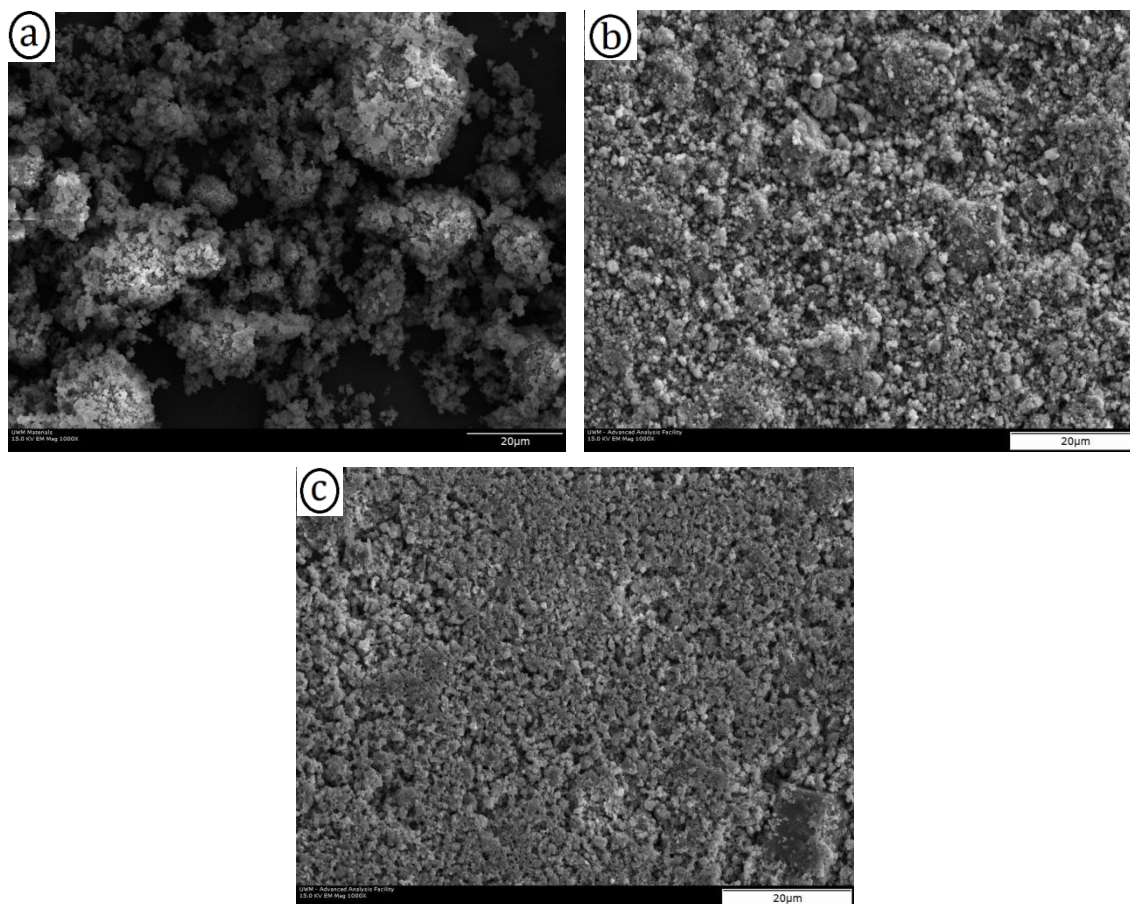


**Figure 31: 1.0 wt% boron milled for 12 hours at 1000x magnification
(a) Before sintering, (b) Sintered for 1 hour, (c) Sintered for 10 hours**

Samples that were milled for 12 hours and sintered for one hour are shown in Figure 32 at 1000x magnification. These pictures give insight to what the topography of how the powders appeared as boron content increases. Figure 32 (c) shows more diversity in appearance than Figure 32 (a), which is mostly uniform. There is a noticeable difference in the sample with zero boron, Figure 32 (a), and the sample with one weight percent boron, Figure 32 (c). Figure 32 (a) has a very uniform appearance to it, with a few larger particles scattered around. Figure 32 (c), however, shows a well mixed sample with smaller boron particles throughout.

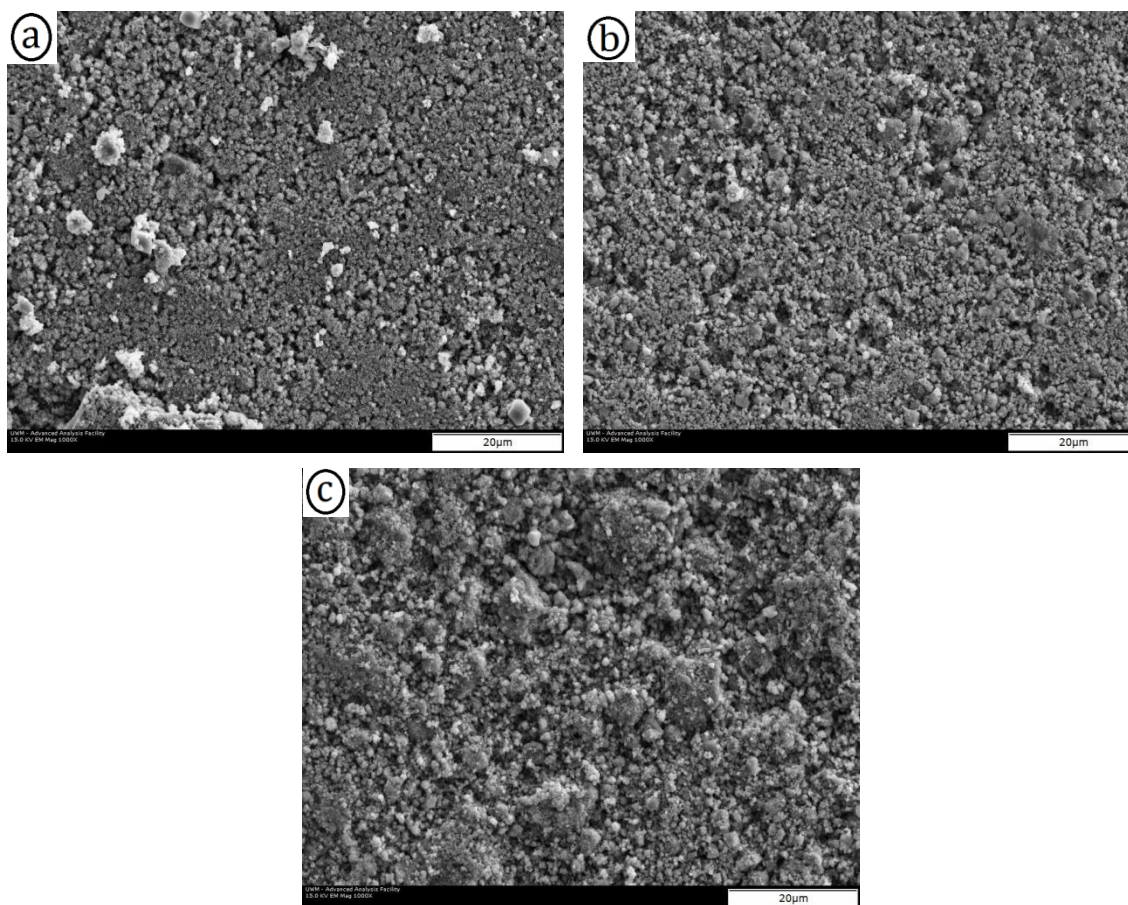


Figure 32: Samples milled for 12 hours and sintered for 1 hour at 1000x magnification
(a) Pure alumina, (b) 0.2 wt% boron, (c) 1.0 wt% boron

Figures 33 and 34 show Sample 19, the 1.0 weight percent boron sample that was hand mixed, viewed at 200x and 1000x magnification, respectively. Sample 19 was observed to have rod-like features. No other sample showed these characteristics. These rod-like structures in the sample are likely due to poor mixing of the sample as described previously. There was possibly a clump of the poorly mixed alumina powder in one area which led to this picture turning out the way it did. Other than the one area shown in Figure 34, this sample had a uniform topography over the entire rest of the pellet. Even though this sample was not ball milled, it must have been mixed well enough for the pellet to remain in one piece after sintering.

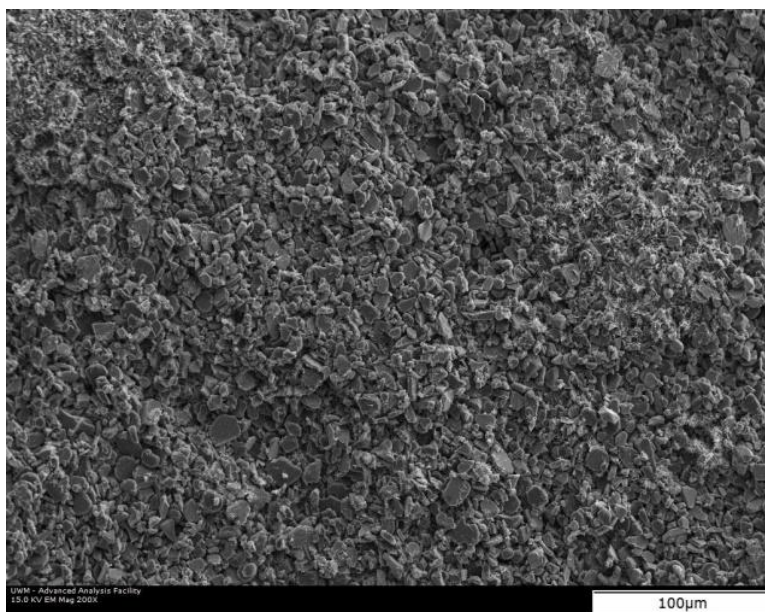
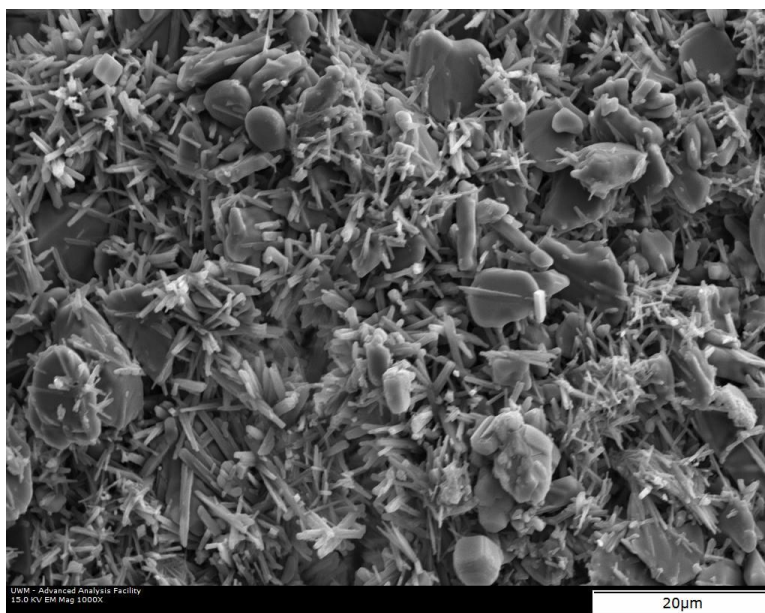


Figure 33: 1.0 wt% boron, hand mixed, sintered for 1 hour at 200x magnification



**Figure 34: Approximate upper-right of Figure 33 at 1000x magnification
Rod-like features exclusive to this sample**

4.3 Porosity

Table 4 shows the sintered samples calculated porosity, the average diameter of the pellets after sintering, and the change in diameter from pre-sintering to post-sintering. The post-sintering diameter was calculated using an average of five measurements. The only sample that did not get five measurements was Sample 23, alumina as-received and sintered for 10 hours, which cracked after being pressed and further cracked after being sintered. Samples 18 and 19 increased in diameter after being sintered for one hour. Sample 18 was 1.0 weight percent boron, milled for 0.3 hours and Sample 19 was 1.0 weight percent boron, hand mixed. This could possibly be attributed to defects or inclusions within the crystal structure. Another cause of this could be a reaction taking place between the alumina and boron that increased volume during sintering.

These samples were likely poorly sintered due to the porosity percentages being relatively high. Sintering at 1200°C could be too low of a temperature to get good densification. Another cause of this poor sintering could be the length of time sintered. Sintering for longer than one hour could perhaps improve the amount of porosity within the samples, although the samples sintered for 10 hours do not have the lowest porosities.

There are also many sources of error that come with this method of porosity measurements. The balance was being supported by lab-jacks and could have perhaps not been perfectly level. The basket being suspended in water also could also provide another large error source. The samples not being fully saturated could cause measurements to be inaccurate as well. Steps were taken in an attempt to produce the most accurate results, but there are still many factors that could affect the porosity

measurements. Even though there are many possible sources of error, the trends should stay relatively the same.

Sample	wt% Boron	Milling Time	Sintering Time	Porosity	Average Post-Sinter Dia. (mm)	Change in Diameter*
16	1	6	1	29.81%	12.60	-0.79%
17	1	3	1	40.63%	12.70	-0.02%
18	1	0.3	1	37.63%	12.77	0.54%
19	1	N/A	1	32.28%	12.79	0.68%
20	0	12	1	43.01%	12.57	-1.01%
21	1	12	1	37.36%	12.54	-1.29%
22	0.2	12	1	39.35%	12.59	-0.83%
23	0	0	10	38.42%	12.66	-0.31%
24	0	12	10	41.02%	12.50	-1.59%
25	1	12	10	38.52%	12.32	-3.02%
26	0.2	12	10	39.16%	12.51	-1.46%

Table 4: Porosity of sintered samples
***Diameter before sintering is assumed to be 12.7mm**

Figure 35 shows the change in diameters of the pellets versus the calculated porosity of the pellets. Each sample is labeled with a sample number on the plot for visibility. Samples 16 through 23 were sintered for one hour. Samples 24, 25, and 26 were sintered for 10 hours. There is no clear trend on how the change in diameter is affected by the porosity of the sample.

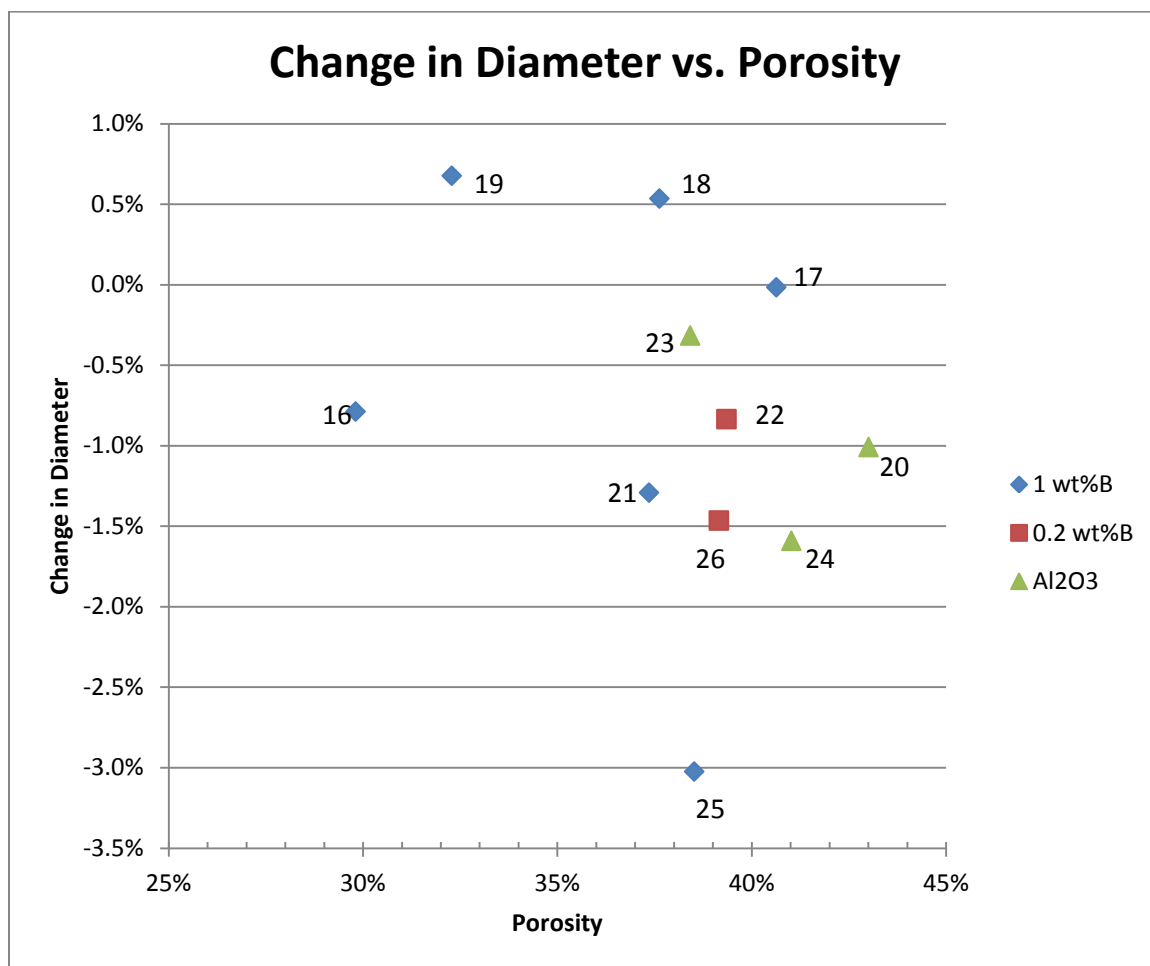


Figure 35: Change in diameter vs. porosity of samples after sintering

Figure 36 shows the porosity of samples with 1.0 weight percent boron as milling time is increased after one hour of sintering. There is no clear trend on how porosity is affected by milling time, as the porosity is increased steadily, followed by a decrease at six hours, and another increase up to 12 hours. To get a better picture on what happens in the gaps, additional samples would need to be tested after being milled for four, eight, and 10 hours. Longer milling times would be required as well in order to see if a trend continues.

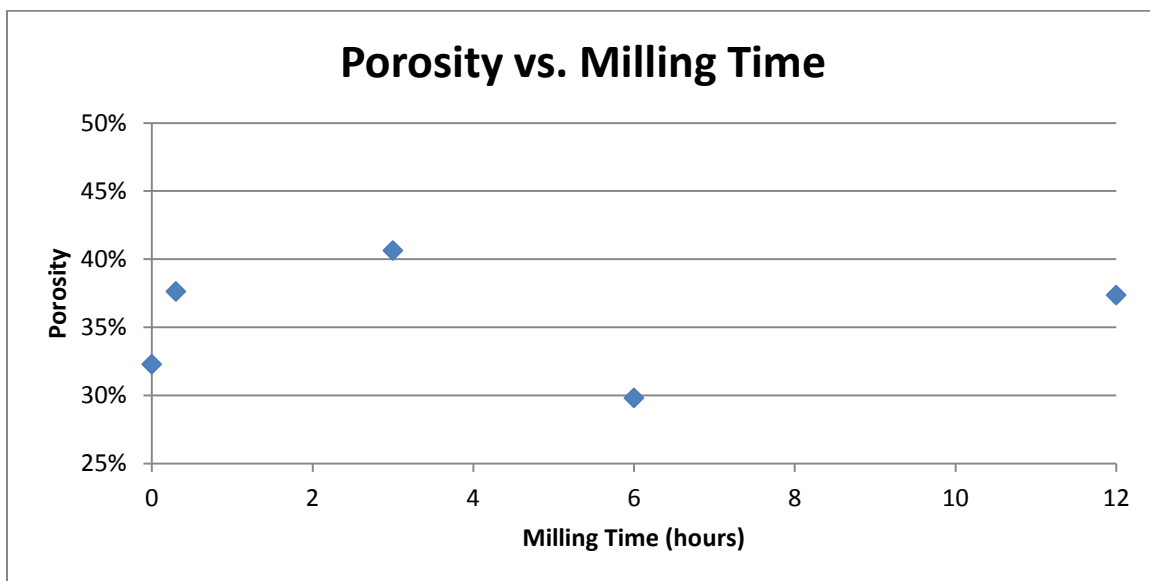


Figure 36: Porosity vs. milling time of 1.0 wt% boron samples after sintering for 1 hour

Figure 37 shows the trends on how porosity is affected by the amount of boron in the samples after sintering for one hour and 10 hours. Both sets of data follow the same trend. A steady decrease from 0.0 to 0.2 weight percent boron is observed followed by shallower slope from 0.2 to 1.0 weight percent boron. Imagining if the plot were extended out to 2.0 or 3.0 weight percent boron, it appears that there would be a leveling off of the slope around 37% for the samples sintered for one hour and 38% for the samples sintered for 10 hours. Larger compositions of boron would be needed to reinforce this idea. The amount of boron appears to have a larger effect on porosity than milling time does, but only to a certain point. To see the full extent of the effects of both milling and boron content, a full range of samples would need to be tested for porosity. These samples are pure alumina, 0.2 weight percent boron, and perhaps 0.6 weight percent boron each milled for 0, 0.3, 3, 6, and 12 hours and sintered for one and 10 hours for a total of 30 samples.

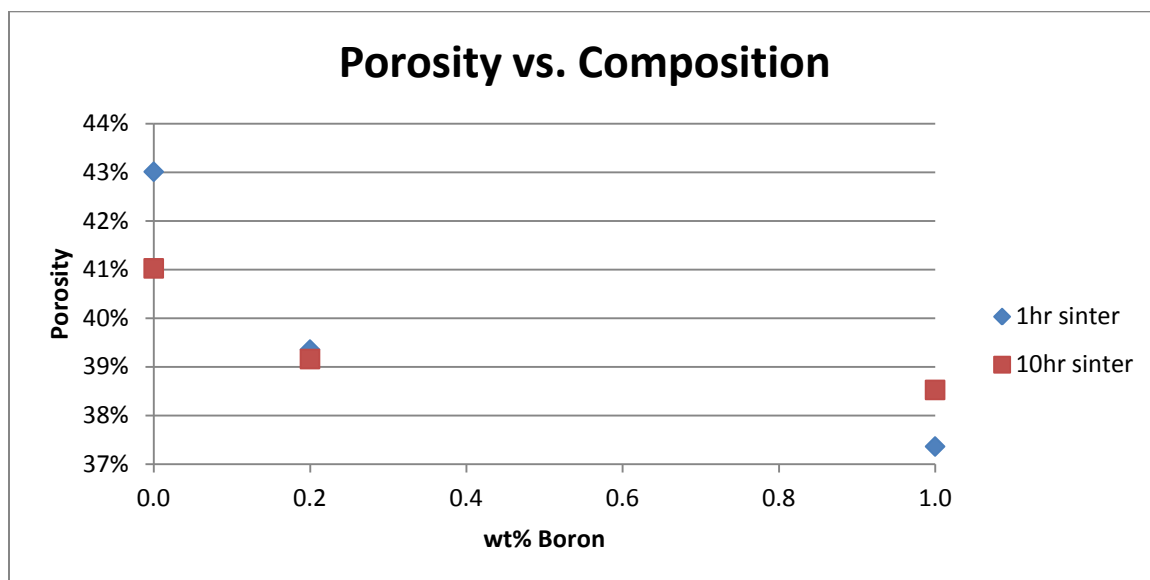


Figure 37: Porosity vs. composition of samples milled 12 hours after sintering for 1 and 10 hours

Figure 38 shows the change in the diameters of the pellets with 1.0 weight percent boron as a function of milling time. There is a near linear decreasing trend as milling time is increased. The slope becomes slightly shallower after six hours of milling. Samples milled for eight and 10 hours would help fill in this gap. Samples milled longer than 12 hours would also have to be tested to see if this trend continues or levels off. This shows that milling time promotes densification.

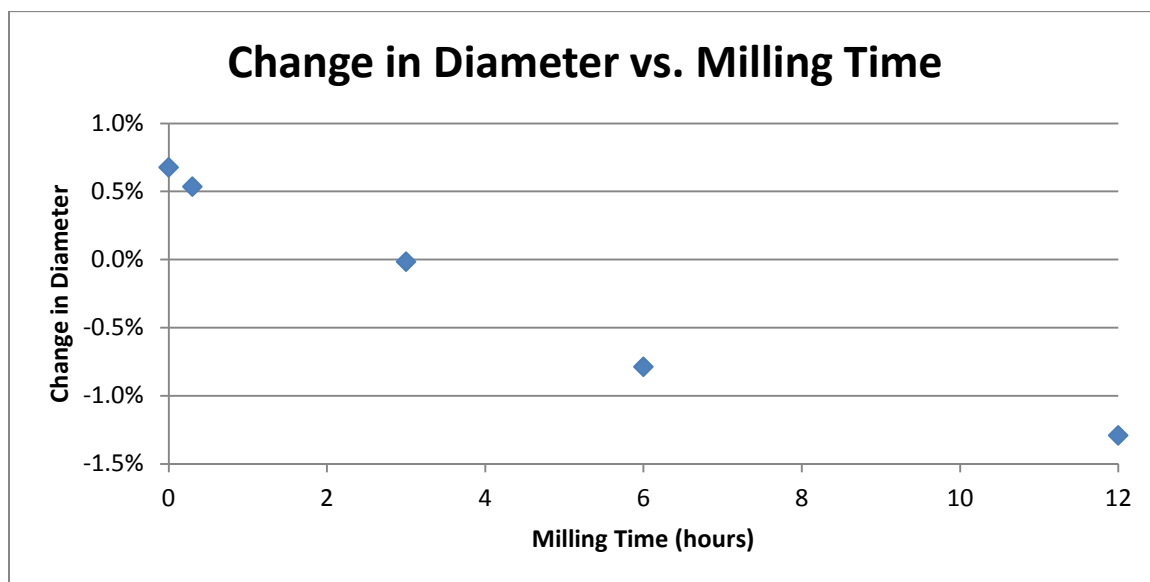


Figure 38: Change in diameter vs. milling time of 1.0 wt% boron samples after sintering for 1 hour

The change in the diameters of the samples that were milled for 12 hours and sintered for one and 10 hours is shown as a function of boron composition in Figure 39. Both sets of samples follow the same trend. Additional samples of 0.4, 0.6, and 0.8 weight percent could be processed to get a better idea of this trend. The samples sintered for 10 hours seem to have a larger effect on the change in diameter. If these trends continue downward at higher boron contents, the boron content will have a larger effect on densification than milling time. Both of these processing variables increase densification during sintering.

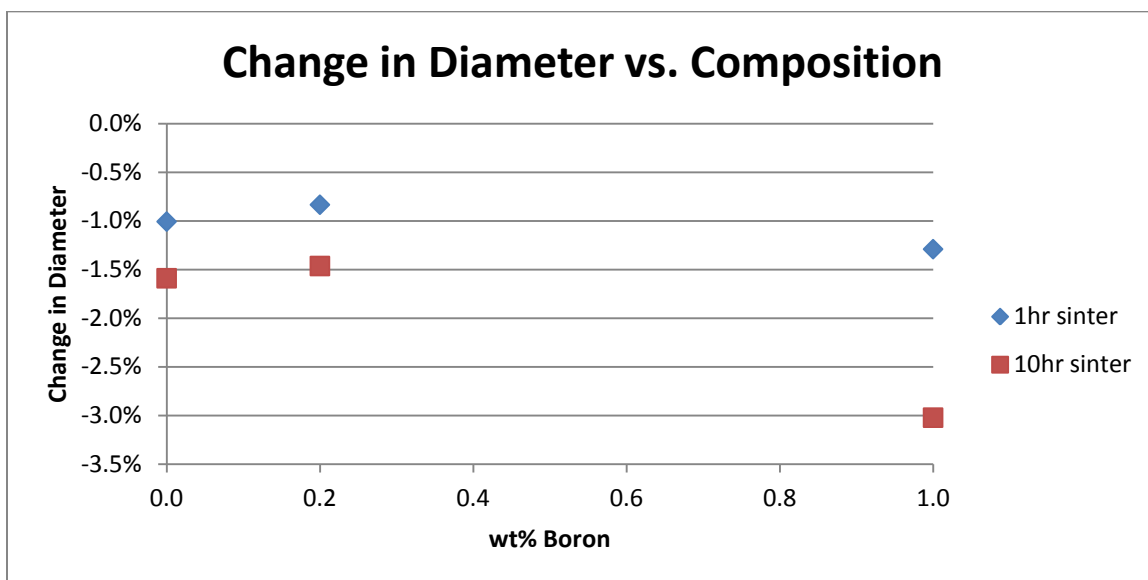


Figure 39: Change in diameter vs. composition of samples milled for 12 hours after sintering for 1 and 10 hours

5. Conclusions

Samples of pure alumina to 1.0 weight percent boron additions were prepared in a high energy ball mill for times up to 12 hours. The XRD patterns show a clear peak broadening as milling time increases, meaning that crystallite size decreases with increases in milling time. Milling samples for about 12 hours appears to be the longest length of time necessary to get the smallest crystallite size. Any more milling time would not further reduce crystallite size appreciably. It is possible that milling for slightly less time, like 10 or 11 hours, would likely produce the same crystallite size results.

After sintering, the crystallite size vs. milling time becomes somewhat random when the Bruker and MAUD results are compared. The randomness could be attributed to the crystallite size being larger than 1000 angstroms, which is larger than the XRD peak broadening effect can be utilized to measure crystal size, making these readings somewhat meaningless. Crystallite size with respect to boron composition shows a trend where the crystallite size levels off between 0.2 and 1.0 weight percent boron.

Before sintering, the lattice parameters do not seem to follow any sort of trend as a function of milling time. This could be attributed to measurement errors in calculating precise lattice parameter values.

The lattice parameters versus milling time start to follow a trend after sintering, however. There is a steady increase of both lattice parameters (a) and (c) from zero to six hours of milling followed by a leveling off up to 12 hours. When the lattice parameters changes to a function of weight percentage of boron, these trends change. Lattice parameters of the samples sintered for one hour follow a relatively flat trend from 0.0 to

1.0 weight percent boron, but the samples sintered for 10 hours decrease from 0.0 to 0.2 and start to level off between 0.2 and 1.0 weight percent boron. The disappearing phase in the 1.0 weight percent boron sample that was milled for 12 hours and sintered for 10 hours suggests that the sintering time could be too long. A reason for lattice parameters to change is a change in composition. So if phase does in fact disappear, that could attribute to the change in both lattice parameters.

Diffraction patterns show a borate phase (aluminum borate - $\text{Al}_{4.9}\text{B}_{1.1}\text{O}_9$) only in the one sample of 1.0 weight percent boron that was milled for 12 hours and sintered for one hour. This phase disappeared after the same sample had been sintered for 10 hours. The 0.2 weight percentage of boron in alumina samples did not affect the samples at all. No additional peaks were observed. If there are additional peaks from the aluminum borate phase, they are too small to detect.

Sintering for one hour reduces the porosity and pellet diameter as expected. 10 hours of sintering may be too long, however, due to a disappearing phase as mentioned previously. While most samples were observed to have a decrease in diameter, samples 18 and 19 were seen to have an increase in their diameters. Samples 18 and 19 are 1.0 weight percent boron samples that were milled for 0.3 hours and hand mixed, respectively, that have been sintered for 1 hour. This could be attributed to defects within the crystal structure or reaction products being produced during sintering. High porosity was observed as well due to a poor sinter. These porosity values could be skewed due to human error, but the trends should remain the same. Samples ranged from 29.81% porosity to 43.01% porosity. The samples with 1.0 weight percent boron added to them tend to have a lower porosity.

The main conclusions from this work can be summarized with the following:

- Before sintering, crystallite size reduction as a function of milling time is the same regardless of the amount of boron being added to the alumina powder
- Pre-sintered lattice parameter changes were found to contradict results presented in literature which indicates that some impurities encountered in the literature processing methods may have had an impact on lattice parameter changes
- Milling of 1.0 wt% boron-containing powders promotes densification during sintering
- Additions of boron promote densification during sintering with a relatively lower porosity
- Both ball milling and 1.0 weight percent boron additions provide the highest densification relative to other samples at sintering times of one and 10 hours

6. Future Work

Milling time is shown to level off once it gets to about 12 hours, so milling longer would not have any additional effects. Also milling for shorter periods of time would not be necessary either due to the fact that smaller particle sizes are desired for this kind of testing.

One area that could be looked into more is the sintering temperature. Testing the samples above 1200°C but well below 1500°C, for example 1300°C, could yield different results.

Sintering for more than 1 hour but less than 10 hours could be another area of interest. By looking at the aluminum borate peaks that disappeared in the diffraction pattern of sample 25, 10 hours of sintering may be too long. Sample 25 was 1.0 weight percent boron, milled for 12 hours and sintered for 10 hours. By sintering for 5 or 6 hours, this could decrease the porosity while keeping the phases that were not present after 10 hours of sintering.

Different amounts of boron could be tested as well. It seemed that 0.2 weight percent boron barely affected the sintering properties, but 1.0 weight percent boron seemed to noticeably affect the results. By trying higher amounts of boron, like 2 or 3 weight percent, the results could perhaps be further affected. However, there could be an upper limit to how much boron can be added, causing detrimental effects past that amount. Testing boron additions between 0.2 and 1.0 weight percent, such as 0.4, 0.6, or 0.8 weight percent, could also potentially provide different results.

One last variable that could be used in future testing is the atmosphere of sintering. The samples in this work were sintering in air, but sintering in a different atmosphere, such as hydrogen, could produce different results.

Material performance, like mechanical properties and wear, could be tested to see how the performance is affected by these processing conditions and how they compare to prior performance results.

Lastly, more samples at each processing variable could be tested to start gathering results for statistical analysis.

7. References

- [1] R. Paluri and S. Ingole. Surface Characterization of Novel Alumina-based Composites for Energy Efficient Sliding Systems. *JOM*. 2011. 63(6). 77-83.
- [2] R. Paluri and S. Ingole. Effect of Composition of Boron on the Tribological Performance of Alumina Matrix Multifunctional Composites for Energy Efficient Sliding Systems. *Processing and Properties of Advanced Ceramics and Composites IV: Ceramic Transactions*. 2012. 234. 279-287.
- [3] M. Demuynck, J. Erauw, O. Van der Biest, F. Delannay, and F. Cambier. Densification of alumina by SPS and HP: A comparative study. *Journal of the European Ceramic Society*. 2012. 32. 1957-1964.
- [4] A. Chakrabarti, L. Kuta, K. Krise, J. Maguire, and N. Hosmane. Boron-Based Nanomaterials Technologies and Applications. 2012. *Boron Science: New Technologies and Applications*. 20. 491-514.
- [5] T. Liu, Q. Li, and S. Fan. Self-catalytic growth of aluminum borate nanowires. *Chemical Physics Letters*. 2003. 375. 632-635.
- [6] I. Gonzalez-Martinez, et al. Defect assisted thermal synthesis of crystalline aluminum borate nanowires. *Journal of Applied Physics*. 2012. 112(024308). 1-5.
- [7] Y. Zhu, Y. Bando, and R. Ma. Aluminum Borate-Boron Nitride Nanocables. *Advanced Materials*. 2003. 15(16). 1377-1379.
- [8] H. J. Goodshaw, J. S. Forrester, G. J. Suaning, and E. H. Kisi. Sintering temperature depression in Al_2O_3 by mechanical milling. *Journal of Material Science*. 2007. 42. 337-345.
- [9] T. Shirai, H. Watanabe, M. Fuji, and M. Takahashi. Structural Properties and Surface Characteristics on Aluminum Oxide Powders. *Ceramics Research Laboratory, Nagoya Institute of Technology*. 2009. 9. 23-31.

- [10] M. Sathiyakumar and F. D. Gnanam. Influence of MnO and TiO₂ additives on density, microstructure and mechanical properties of Al₂O₃. *Ceramics International*. 2002. 28. 195-200.
- [11] T. Yadav, R. Yadav, and D. Singh. Mechanical Milling: a Top Down Approach for the Synthesis of Nanomaterials and Nanocomposites. *Nanoscience and Nanotechnology*. 2012. 2(3). 22-48.
- [12] N. Salah, et al. High-energy ball milling technique for ZnO nanoparticles as antibacterial material. *International Journal of Nanomedicine*. 2011. 6. 863-869.
- [13] P. Balaz. High-Energy Milling. *Mechanochemistry in Nanoscience and Minerals Engineering*. 2008. 2. 103-132.
- [14] G. R. Karagedov and N.Z. Lyakhov. Mechanochemical Grinding of Inorganic Oxides. *KONA*. 2003. 21. 76-87.
- [15] T. Ekström, C. Chatfield, W. Wruss, and M. Maly-Schreiber. The use of X-ray diffraction peak-broadening analysis to characterize ground Al₂O₃ powders. *Journal of Materials Science*. 1985. 20. 1266-1274.
- [16] G. Scholz, et al. Local structural orders in nanostructured Al₂O₃ prepared by high-energy ball milling. *Journal of Physics: Condensed Matter*. 2002. 14. 2101-2117.
- [17] L. Lutterotti, S. Matthies, and H. R. Wenk. MAUD (Material Analysis Using Diffraction): a user friendly Java program for Rietveld Texture Analysis and more. *Commission for Powder Diffraction*. 1999. 21.
- [18] L. Lutterotti. Introduction to Diffraction and the Rietveld Method. *Laboratorio Scienza e Tecnologia dei Materiali*.
<http://www.ing.unitn.it/~luttero/laboratoriomateriali/RietveldRefinements.pdf>